U.S. OFFICE OF NAVAL RESEARCH

GRANT N00014-91-J-1629

R&T Code 413S001

Technical Report #20

An atomically-resolved STM study of the Thermal Decomposition of Disilane on Si(001)

by

Y. Wang, M. Bronikowski, and R.J. Hamers

Prepared for Publication

in

Surface Science

May 10, 1993

Department of Chemistry
University of Wisconsin-Madison
Madison, WI 53706

DISCLAIMER NOTICE

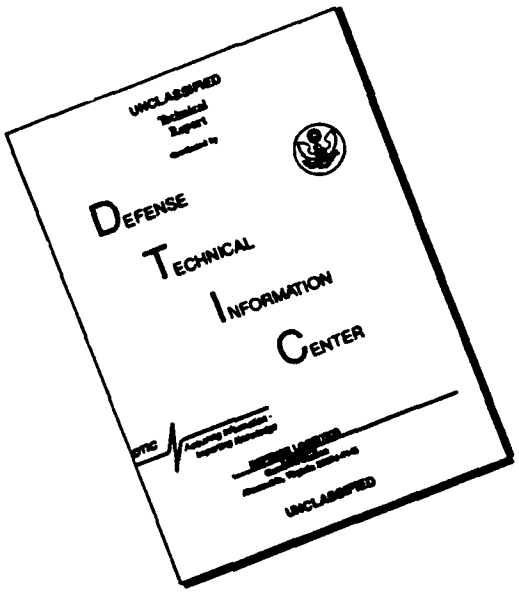

THIS DOCUMENT IS BEST QUALITY AVAILABLE. THE COPY FURNISHED TO DTIC CONTAINED A SIGNIFICANT NUMBER OF PAGES WHICH DO NOT REPRODUCE LEGIBLY.

REPORT DOCUMENTATION PAGE

Form Approved
OMB No. 0704-0188

1. AGENCY USE ONLY (Leave blank)	2. REPORT DATE	3. REPORT TYPE AND DATES COVERED
	5/27/94	Interim 6/1/93-5/31/94

4. TITLE AND SUBTITLE
An Atomically-Resolved Scanning Tunneling Microscopy Study of the Thermal Decomposition of Disilane on Si(001)

5. FUNDING NUMBERS
Grant
N00014-91-J-1629
R&T Code
413S001

6. AUTHOR(S)
Y. Wang, M. J. Bronikowski and Robert J. Hamers

7. PERFORMING ORGANIZATION NAME(S) AND ADDRESS(ES)
Department of Chemistry
University of Wisconsin-Madison
1101 University Avenue
Madison, WI 53706-1396

8. PERFORMING ORGANIZATION REPORT NUMBER

9. SPONSORING/MONITORING AGENCY NAME(S) AND ADDRESS(ES)
Office of Naval Research, Chemistry
800 North Quincy Street
Arlington, VA

10. SPONSORING/MONITORING AGENCY REPORT NUMBER
20

11. SUPPLEMENTARY NOTES

12a. DISTRIBUTION/AVAILABILITY STATEMENT
Unlimited

12b. DISTRIBUTION CODE

13. ABSTRACT (Maximum 200 words)

Scanning Tunneling Microscopy (STM) has been used to study the adsorption and thermal dissociation of disilane (Si_2H_6) on the Si(001) surface. At low coverage, disilane adsorbs dissociatively to produce adsorbed SiH_3 groups which are randomly distributed on the surface. STM images show that these SiH_3 groups spontaneously dissociate into SiH_2 and H within several minutes of adsorption at room temperature, and images depicting individual dissociation events have been obtained. Thermal annealing leads to diffusion and dissociation of the SiH_2 groups through an intermediate which consists of a hydrogenated dimer which has its dimer axis parallel to those of the underlying substrate, instead of rotated. The structure and chemical identity of the intermediates are discussed in terms of the overall dissociation mechanism. Diffusion of hydrogen atoms leads to the formation of segregated surface phase of clean Si and the Si(001)-(2x1) "monohydride" structure, and bias-dependent STM imaging permits these species to be identified on a dimer-by-dimer basis. At low temperatures the monohydride distribution is non-statistical, showing a preference for flat terraces over small epitaxial islands. The diffusion, desorption, segregation of hydrogen and its role in blocking diffusion of silicon atoms is also discussed.

14. SUBJECT TERMS

15. NUMBER OF PAGES

16. PRICE CODE
---

17. SECURITY CLASSIFICATION OF REPORT	18. SECURITY CLASSIFICATION OF THIS PAGE	19. SECURITY CLASSIFICATION OF ABSTRACT	20. LIMITATION OF ABSTRACT
Unclassified	Unclassified	Unclassified	UL

An Atomically-Resolved Scanning Tunneling Microscopy Study of the Thermal Decomposition of Disilane on Si(001)

Yajun Wang, Michael J. Bronikowski and Robert J. Hamers*

Department of Chemistry, University of Wisconsin

1101 University Avenue

Madison, WI 53706

Phone: 608-262-6371

FAX: 608-262-0453

E-mail: HAMERS @ BERT.CHEM.WISC.EDU

ABSTRACT

Scanning Tunneling Microscopy (STM) has been used to study the adsorption and thermal dissociation of disilane (Si_2H_6) on the Si(001) surface. At low coverage, disilane adsorbs dissociatively to produce adsorbed SiH_3 groups which are randomly distributed on the surface. STM images show that these SiH_3 groups spontaneously dissociate into SiH_2 and H within several minutes of adsorption at room temperature, and images depicting individual dissociation events have been obtained. Thermal annealing leads to diffusion and dissociation of the SiH_2 groups through an intermediate which consists of a hydrogenated dimer which has its dimer axis parallel to those of the underlying substrate, instead of rotated. The structure and chemical identity of the intermediates are discussed in terms of the overall dissociation mechanism. Diffusion of hydrogen atoms leads to the formation of segregated surface phase of clean Si and the Si(001)-(2x1) "monohydride" structure, and bias-dependent STM imaging permits these species to be identified on a dimer-by-dimer basis. At low temperatures the monohydride distribution is non-statistical, showing a preference for flat terraces over small epitaxial islands. The diffusion, desorption, segregation of hydrogen and its role in blocking diffusion of silicon atoms is also discussed.

*Author to whom correspondence should be addressed

INTRODUCTION

Epitaxial growth of silicon on Si(001) has received wide attention due to its importance in the semiconductor industry and as a prototype system for understanding epitaxial growth. While a number of recent studies have intensively studied the atomistics of solid-phase, or "molecular-beam" epitaxy, comparatively little attention has been paid to understanding the atomistics involved in growth from chemical precursors, widely utilized in chemical vapor deposition (CVD) techniques. Recent studies have shown that device-quality epitaxial films can be grown a temperatures much lower than conventional CVD reactors provided that the surfaces are maintained scrupulously clean[1]. The development of such "ultra-high vacuum", or "UHV-CVD" techniques has motivated an increased understanding of the surface chemistry of CVD precursors at temperatures of 400-700 Kelvin. While a number of different precursors such as SiH_4[2, 3], SiH_2Cl_2[4-6] and Si_2H_6[7] have been used for epitaxial growth, Si_2H_6 is a particularly promising precursor for low-temperature epitaxy because the low energy of the Si-Si bond leads to a high sticking coefficient without the presence of chlorine[8] .

The decomposition of disilane on Si(001) has been widely studied by a number of groups and experimental techniques [9-19]. Diffraction techniques have been used extensively by Joyce and co-workers[13, 14, 20-22] to monitor the surface reconstruction, growth anisotropy, and growth dynamics of Si on Si(001) from Si_2H_6. Gates, et al.[8, 10, 11, 23-34] have done the most extensive work on the decomposition of Si_2H_6 on both the Si(001)-(2x1) and Si(111)-(7x7) surfaces using a variety of mass spectroscopy techniques including temperature programmed desorption(TPD), static secondary-ion mass spectroscopy (SSIMS), and time-of-flight mass spectroscopy (TOF-MS). On the basis of these investigations, they derived the basic chemical scheme of the epitaxy process as:
$Si_2H_6(g) \rightarrow Si_2H_6(precursor) \rightarrow SiH_3(ads) \rightarrow SiH_2(ads) \rightarrow SiH(ads) \rightarrow Si(epitaxial)$
and studied the kinetics of the intermediate steps in the decomposition. Using ultraviolet photoemission spectroscopy(UPS) and TPD, Bozso, et al.[35] studied the Si_2H_6/Si(001) system at temperatures down to 140 K and showed that SiH_3 decomposes above 525K to give H_2 and a monohydride-like Si-H surface layer. A similar pathway, in which a SiH_2 "dihydride"-like specie decomposes to a

Si(001)-(2x1)-H monohydride phase followed by H_2 desorption from the monohydride phase was also suggested by Y. Suda et al[36] from electron energy-loss (EELS) and reflection high-energy electron diffraction (RHEED) results. Lubben, et al.[37] investigated the influence of ultraviolet radiation on the dissociation kinetics of Si_2H_6 under conditions appropriate for atomic layer epitaxy. The interaction of hydrogen with the Si(001) surface has also received widespread attention due both to its importance in controlling the rate of CVD reactions and as a model chemical adsorbate system[38-48].

While previous studies of hydrogen and disilane interactions with Si(001) have been useful in identifying many aspects of the CVD process, they leave many questions unanswered. For example, many of the experimental techniques cannot distinguish isolated, adsorbed molecular fragments of SiH from the ordered Si(001)-(2x1)H monohydride which forms on extended terraces, despite the fact that the two are clearly distinct chemical entities. Likewise, local ordering, bonding geometries and spatial corre'ations between the positions of various adsorbed fragments cannot be readily analyzed using these spatially-averaging techniques.

The desire to better understand the CVD process from a microscopic viewpoint has motivated several studies using scanning tunneling microscopy and tunneling spectroscopy. The initial study of disilane decomposition on Si(001) by Boland[16] focused on the role of hydrogen in controlling the adsorption and dissociation of disilane at high coverage, showing that under these conditions epitaxial growth is driven by the decomposition of the fragments produced by disilane adsorption on the clean Si(001) surface. Using STM to investigate the interaction of atomic hydrogen with the Si(001) surface, Boland showed that the hydrogen atoms produced by direct adsorption of H atoms[49, 50] or from dissociation of disilane[16] pair up to form a Si(001)-(2x1)-H monohydride before the desorption, and suggested that this hydrogen pairing was responsible for the first-order desorption kinetics of hydrogen on Si(001)-(2X1) surface which was widely known from earlier TPD studies. Lin, et al[15] also used STM to study the adsorption of Si_2H_6 at 623K, observing the formation of anisotropic islands; they assigned these islands to Si(001)-(2x1)-H monohydride, suggesting that the island nucleation occurred before full dissociation or randomization of the hydrogen atoms. Their studies showed

that fragments from the initial adsorption of Si_2H_6 were randomly distributed on the surface, but no information about the nature of the dissociation fragments was reported. In an effort to determine the identity and bonding locations of the dissociation fragments, Bronikowski, et al.[51] performed a detailed study of disilane adsorption at room temperature with submonolayer coverage in which we showed that room temperature adsorption of Si_2H_6 gives almost exclusively adsorbed SiH_2 fragments and adsorbed hydrogen atoms, with the former located in a bridge-bonded site between two dimers with a dimer row, and with the latter bonded on one of the "dangling bonds" of the Si(001) dimers.

While these previous STM studies have emphasized on the initial and final products of the reactions of disilane on Si(001), they have not addressed the important mechanistic question of *how* this decomposition occurs. In this study, we report a detailed investigation of the adsorption and the thermal decomposition of the disilane on the Si(001) surface. By dosing the surface with disilane at room temperature and using bias-dependent imaging to probe the atomic-scale chemical nature at successively higher temperatures, we have mapped out the relevant chemical transformations and have established the identity, bonding locations and spatial correlations of a number of intermediate species such as SiH_3(ads), SiH_2(ads), H(ads), H-Si-Si-H(ads), paired H(ads), DB-Si-Si-H(ads)(DB=dangling bond) and several types of distinguishable adsorbed Si=Si dimers. We have also identified conditions under which the monohydride phase, formed by pairing of hydrogen atoms on a single dimer, can be identified unambiguously on a dimer-by-dimer basis, and we show that the monohydride phase is found preferentially on flat terraces and is less favored on small silicon islands. Our detailed studies of the chemical composition of the surface contradict findings obtained in two earlier brief studies of this system, demonstrating the importance of understanding the STM imaging process and with important implications for understanding the decomposition mechanism.

EXPERIMENTAL

STM experiments were performed in an ultrahigh vacuum (UHV) chamber with a base pressure of less than 10^{-10} torr. The STM consists of a

single-tube scanner mounted at the end of a Burleigh "Inchworm". All feedback and inchworm control electronics[52] were home-made. The microscope hangs from springs inside an ultrahigh vacuum chamber equipped with a load-lock for exchanging both samples and tips. To avoid sample contamination, no thermocouple or other materials containing transition metals other than molybdenum or tantalum were allowed near the sample. Samples were resistively heated on a separate heating stage by passing DC current through the sample. Temperatures greater than 875 K were directly measured using an optical pyrometer, while temperatures below 875 K were determined using an ex-situ temperature calibration as follows. During experiments, the power dissipated in the sample was determined as the product of the applied voltage and current. After finishing experiments with a given sample, the sample and its entire holder were removed from the UHV system, and then a 0.075 millimeter chromel-alumel thermocouple was attached to the back of the sample using a small amount of Ultratem 516 high-temperature cement; the sample holder assembly and thermocouple were then introduced back into the UHV system, and the temperatures were calibrated by plotting the thermocouple reading vs. the power dissipation. Using this method, temperatures are believed to be reliable to within 30 Kelvin.

N-type Si(001) wafers oriented to within 0.5^{o} (Virginia Semiconductor) were used. Clean Si(001)-(2X1) surfaces were achieved by degassing for 10-12 hours at 920-970K, then heating to 1425K for several seconds while maintaining the chamber pressure in the mid-10^{-10} torr pressure range. After cooling to room temperature (about 30 min), the samples were exposed to 10% Si_2H_6 in He (Voltaix, Inc) through a leak valve. Coverages were controlled by varying the pressure and exposure time; all exposures stated in this paper are corrected for the He dilution and refer to actual exposures of disilane. Because the only significant impurity in disilane is silane and the latter has a much smaller sticking coefficient[8, 25], disilane can be used without further purification. Dosing experiments were performed either by dosing the sample before transferring to the STM tunneling stage, or by exposing the sample directly on the tunneling stage. The former approach gives more reproducible coverages and was used for most of the experiments reported here. However, experiments were also performed in which the sample was dosed while tunneling, providing sequential images of the same

area at different exposures. Such experiments are crucial in properly identifying the role of defects and other inhomogeneities in the CVD process and have even permitted us to observe in an unambiguous way the dissociation of *individual* molecular fragments.

All images were acquired in the constant current mode using tunneling currents between 0.1 and 1.0 nA and a range of bias voltages between 1.2 and 3 Volts at both positive sample bias (probing empty surface states) and negative sample bias (probing filled surface states). Since it has been demonstrated that the STM tip can induce chemistry at high voltages and/or current[53], we performed control experiments to ensure that the behavior we observe is not induced by the tip. Our control experiments show that voltages as high as 3 volts and currents as high as 6 nA have no effect on the surface. Since in our experiments we usually use smaller voltages(around 2V) and typically use much lower currents on the order of 0.3 nA, we believe all surface features reported here are intrinsic to the surface, and the STM can be assumed to be a non-intrusive probe of the surface geometric and chemical structure.

RESULTS

Section I: Adsorption at 300 Kelvin:

Figure 1a shows an STM image of a Si(001) surface before dosing with disilane. The Si(001) surface reconstructs by a pairing mechanism, forming rows of dimers on the surface[54-56]. The electronic structure of the dimer can be understood as resulting from a rehybridization of the two "dangling bonds" on each of two covalently-bonding silicon atoms to form σ-bonding, σ^*-antibonding, π-bonding, and π^*-antibonding states[57, 58]. Because the σ and σ^* states lie far from the Fermi level, tunneling electrons primarily access the occupied π state at negative sample bias and the unoccupied π^* state at positive sample bias. At negative bias STM images show the dimers as bean-shaped structures arranged in rows, while at positive bias the nodal plane of the π^* state reduces the local density of unoccupied states, leading to a depression in the center of the dimer bond and a pronounced "splitting" of the dimer into two well-resolved protrusions[59]. Consistent with previous studies, the surface also contains some defects; the structure and properties of these defects have been treated in detail previously[56]. Finally, we note that two

types of step edges are clearly shown in fig. 1a and 1b; type "A" steps are defined as those in which the step edge runs parallel to the rows of dimers on the upper terrace. Type "B" steps are defined as those in which the step edge runs perpendicular to the rows of dimer on the upper terrace. Type "B" step edges have two possible terminations, both of which are observed in STM studies[55]. Type "A" steps tend to be straight, while type "B" edges tend to be rough[60-62].

Figure 1b shows the identical area after exposure to 0.1 Langmuir of disilane. Comparing figures 1a and 1b, two main changes are found. The most obvious change upon exposure to disilane is the appearance of small protrusions (appearing as white circles in the grayscale STM image), several of which are pointed out by arrows in fig. 1b. A second, less obvious change is that in some of the regions which were defect-free and showed only symmetric dimers before exposure to disilane, small atomic-sized vacancies are now observed; the dimers adjacent to these atomic-sized depressions are tilted, leading to a "zig-zag" structure emanating away from the atomic-sized depressions. One such feature is indicated in figure 1b. A further comparison of fig. 1a and 1b shows that the adsorption-induced changes are randomly distributed across the surface and do not show any strong preference for occurring either near defects on the terraces or near any step edges. This demonstrates that surface defects do not play an important role in the initial adsorption of disilane on Si(001), which is consistent with previous studies [15, 16, 51].

As we reported in a previous publication[51], the fragments resulting from adsorption and dissociation of disilane on Si(001) can be identified using STM images acquired at different voltages, determining the locations of the observed features with respect to the underlying crystal lattice (thereby determining their surface coordination), and using simple rules of valence to relate the coordination to the chemical identity. For example, by studying the locations of the bright white protrusions in fig. 1b with respect to the underlying Si=Si dimers, we have determined that the protrusions are found midway between two dimers within a single dimer row, in an off-center position which is neither atop the dimer rows nor midway between the dimer rows. An adsorbate at this location has two bonds to the surface, leading us to

attribute these features to adsorbed SiH_2 groups. Figure 2a and 2b are high-resolution images acquired at +2.0 and -2.5 V respectively, showing that the SiH_2 groups appear as protrusions at -2.5 V when probing filled states but as depressions at +2.0 V when probing empty states, while adsorbed H atoms appear as depressions over then entire range of voltages between -2.5 V and +2V sample bias. Figure 2c shows the corresponding surface model for the assignment of those adsorption-induced features. The identification of adsorbed hydrogen atoms is based on previous work by Boland[45, 63] of hydrogen adsorption on Si(001) and is consistent with our previous study of disilane adsorption on Si(001)[51]. Both these studies showed that adsorption of H on a dimerized silicon atom breaks the dimer π bond; this reduces the density of states near the Fermi energy E_F on the atom to which the H atom is bonded, but increases the state density near E_F on the other atom of the dimer, which becomes essentially a surface radical with an unpaired electron. As a result, the H atom appears as a depression but the "dangling bond" produced on the other Si atom of the dimer pair appears as a protrusion because electrons can easily tunnel both in to and out of this partially-filled dangling bond. In addition, adsorption on one H atom on a Si dimer pair breaks the mirror-plane symmetry of the dimer, inducing a buckling (or tilting) of the dimers. As noted previously, the direction of dimer tilting around localized defects on Si(001) alternates from dimer to dimer and produces a zig-zag pattern which is visible in fig. 1b. Note that scanning over a single area at different bias voltages, one can clearly and unambiguously establish the correlation between negative- and positive-bias images.

At low coverages, images such as fig. 1b show that the predominant surface species are adsorbed H atoms and adsorbed SiH_2 groups. Previous studies[15, 29, 36, 37] have suggested several possible reactions for the initial disilane decomposition, including (a) $Si_2H_6 \rightarrow SiH_4(gas) + SiH_2(ads)$; (b) $Si_2H_6 \rightarrow 2SiH_2(ads) + 2H(ads)$; and (c) $Si_2H_6 \rightarrow 2SiH_2(ads) + H_2(gas)$. The relative importance of these three reactions can be determined from an analysis of the ratio of SiH_2 groups to H atoms on the surface. The number of SiH_2 groups and the number of adsorbed H atoms within the same area were counted on several atomically-resolved images (such as fig. 1b), each image having an area of 250,000 $Å^2$. These counting results show that at coverages of 0.1 or less the ratio of $SiH_2(ads)$ to H(ads) is 1.0 ± 0.1, indicating that the predominant surface

reaction involved in the dissociation is $Si_2H_6 \rightarrow 2SiH_2(ads) + 2H(ads)$ in this low coverage regime with no hydrogen loss to the vacuum.

While at low coverage the surface consists of adsorbed SiH_2 groups and H atoms, as the surface concentration becomes higher the number of available surface sites becomes smaller, and the dissociation probability of the silicon hydrides is reduced[26]. As a result, at high coverages surface species such as SiH_3 are expected to be more prevalent. STM images of surfaces exposed to disilane at higher coverage show that SiH_3 groups are indeed initially formed on this surface, but at low coverage are unstable and dissociate to SiH_2 groups and adsorbed H atoms on a time scale of tens of minutes. Figure 3 shows sequential scans of one particular surface area as a function of disilane exposure. Fig. 3a was obtained after 0.1 Langmuir exposure, while successive images were obtained approximately 230 seconds apart while maintaining a background pressure of 1.5×10^{-8} torr. Again, the images show that adsorption is random with no preference for steps or defects. At the lowest coverages, analysis of the bonding locations shows that adsorbed SiH_2 groups and adsorbed H atoms are the only surface species present. At higher coverages, however, fig. 3c shows several examples of a new feature which again appears as a protrusion, but is clearly distinguishable from the SiH_2 groups from its apparent height and from its bonding symmetry. Two examples of this new feature are indicated by the arrows in fig. 3c. At -2.2 V sample bias, this new feature appears approximately 0.5 Å higher than the SiH_2 groups (thereby also making it look slightly larger than the SiH_2 groups in a grayscale image). High-resolution images (below) show that this fragment is bonded directly on one of the terminal "dangling bonds" of a Si=Si dimer, rather than the bridge-bonded position characteristic of the SiH_2 groups. Since this terminal "dangling-bond" position is exactly where an SiH_3 fragment would be expected to bond in order to achieve four-fold tetrahedral coordination, we attribute these new features to adsorbed SiH_3 groups. This conclusion is confirmed by direct observation of the dissociation of SiH_3 groups, as discussed below.

At very high coverage it becomes difficult to determine the bonding locations of all surface species, but our experiments indicate that a substantial fraction of the adsorbed species are SiH_3 groups. The surface shown in fig. 3f

has been completely saturated, and sequential images after even much higher exposure show no further changes, indicating that no more adsorption takes place. Although in principle one SiH_3 group can bond to each end of each dimer on the surface, thereby achieving a total coverage of one monolayer, this does not occur in practice. Annealing surfaces such as fig. 3f produces silicon islands which cover only approximately 33% of the surface; this indicates that either a substantial fraction of the surface sites are covered with hydrogen from SiH_3 dissociation, or else that steric hindrance between SiH_3 groups restricts adsorption at high coverage, as noted previously by Boland[16] and by Lubben, et al.[37]

The chemical composition of the surface is not only dependent on coverage, but can also change with time. Indeed, perhaps the most convincing and exciting proof of our identification of the SiH_2 and SiH_3 species lies in images which directly show the spontaneous dissociation of an SiH_3 group into an SiH_2 group plus a hydrogen atom! Figure 4 shows three sequential images of one particular area of the surface. Fig. 4a shows the area before dosing, revealing symmetric-looking dimers and two small vacancy defects at left. After fig. 4a was obtained, the tip was retracted about two microns, and the sample was dosed with 0.1 Langmuir disilane. The tip was then brought into the tunneling regime again, and the image in fig. 4b. was obtained. In this image, two molecular fragments can be observed. One fragment, labeled "SiH_2", is in the bridge-bonded position typical of an adsorbed SiH_2 group, while the second fragment is on a "dangling-bond" site characteristic of an adsorbed SiH_3 group. Approximately 8 minutes later, the image shown in fig. 4c was obtained. Comparing fig. 4c to 4b shows two changes. First, we note that the fragment previously located on a "dangling bond" site and attributed to an SiH_3 group is now located on a bridge-bonded site characteristic of an SiH_2 group. Secondly, we note the appearance of an atomic-sized depression surrounded by tilted dimers, which is the characteristic appearance of a lone hydrogen atom adsorbed on the dangling bond of a dimer. *In effect, this image shows the dissociation of an SiH_3 group into an adsorbed SiH_2 group and an adsorbed H atom.* Because the images in fig. 4 were clipped from much larger images which also show the entire surrounding region through this sequence, it is possible to rule out other diffusion or reaction events as the source of the observed changes. Likewise, while we cannot completely rule

out the possibility of the STM inducing this reaction, we note that at low coverage adsorbed SiH_3 groups have only been observed in experiments in which the surface is dosed while tunneling; sequential experiments in which the surface is dosed well in advance of the tunneling experiment show only SiH_2 groups and H atoms. This suggests that at low coverage adsorbed SiH_3 groups are metastable, with a lifetime on the order of minutes. More work to further determine the lifetime of this dissociation is forthcoming.

Section II: Thermal decomposition at low coverage

By acquiring STM images after dosing and then again after annealing the dosed surfaces to elevated temperatures, we are able to identify the chemical and structural changes induced on the surface. Figure 5a shows an image obtained after annealing a disilane-dosed Si(001) surface to 470 K. A comparison of this image with those obtained before annealing shows several changes. The first change is that no SiH_3 groups are visible and although SiH_2 groups are clearly present, their number is reduced due to dissociation. In addition, we find the appearance of four new types of surface species. While decomposition of SiH_2 might be expected to produce SiH as an intermediate, none of the species we observe can be attributed to an adsorbed SiH group. Instead, each of the four new surface species appears to arise from the dimerization of silicon-containing species into different bonding geometries. Three of these four new species can be observed in high resolution in fig. 5b.

In principle, a single dimer can adsorb on the Si(001) surface in four ways, as shown in figure 6. Assuming that the two atoms within the dimer can form both a σ and π bond, each configuration effectively achieves four-fold coordination for the Si atoms in the adsorbing dimer. The energies of a dimer in each of these configurations have been predicted theoretically by Brocks[64, 65] and will be discussed later. Two of these four configurations are found in the normal epitaxial growth of continuous overlayer of silicon on Si(001); here, the bulk crystallography forces the direction of dimerization of the growing layer to rotate by 90 degrees with respect to that of the underlying layer. Because of the dimerization of the original surface, there are two nonequivalent sites on which a dimer can bond, shown in fig. 6b and 6d. The geometries indicated in fig. 6a and 6c can occur for individual

adsorbed dimers, but cannot give rise to continuous overlayers in the form of dimerized Si islands.

By examining the locations of the features observed in fig. 5b with the underlying dimers, we find that the specie labeled "A" appears to be a Si=Si dimer which is bonded directly on top of two dimers within a single dimer row, in an "atop" site, in a geometry like that shown in fig. 6b. The specie labeled "T" appears to be a Si=Si dimer which is located in the "trough" site between two dimer rows, where it can form a total of four bond to the substrate by forming one bond to each of four substrate dimers, as shown in fig. 6d. Dimers in the "A" geometry also appear to be 0.5±0.1 Å higher than dimers in the "T" geometry. It should also be noted that the local bonding observed for these two species is similar to that encountered at type B step edges of slightly-miscut Si(001) surfaces, which show two terminations[66]. In one step termination, often referred to as the "rebonded" geometry, the last dimer of the upper terrace is bonded directly into a dimer of the lower terrace in a geometry comparable to individual dimers of the "T" configuration, while the "non-rebonded geometry has a geometry comparable to dimer in the "A" configuration. Previous STM images of step edges[55] have shown both types of step terminations occur with comparable probabilities, in agreement with our observations which show that dimers in "atop" and "trough" configurations have comparable energies and readily coexist.

A similar analysis of the specie labeled "NRD" in fig. 5b shows that it appears like a dimer centered in the trough between two dimer rows and located midway between dimers in a site of four-fold symmetry, with the dimer axis *parallel* to those of the substrate dimers, a geometry like that shown in fig. 6c. Such "non-rotated" dimers, labeled "NRD" in figs. 5 and 6, appear to be about the same height as the "T" dimer, 0.5 Å below the height of the "A" dimers. As will be discussed later, we believe that the observation of the unusual "NRD" dimer configuration provides insight into the mechanism of dissociation of the adsorbed SiH_X fragments.

We have occasionally observed a fourth type of dimer structure with the same symmetry as the "NRD" dimer, but which appears lower in height and with an obvious splitting at the center of the dimer, as shown in figure 7a & b

and labeled with "NRMH". While it will be shown in detail in next section, we note that for dimers in the more common "A" and "T" orientations (i.e., rotated 90 degrees from the underlying substrate dimer), dimers of "clean" silicon Si=Si and dimers of the monohydride phase H-Si-Si-H can be readily distinguished because dimers of Si=Si are bean-shaped and appear higher, while dimers of H-Si-Si-H show a splitting along the center and appear to be 1.0-1.2 Å lower. The behavior we observed for the "NRD" and "NRMH" dimers mirrors the behavior of the "normal" and "monohydride" dimers. Therefore, we attribute the "NRD" structure to a dimer of clean Si, and we attribute the "NRMH" feature to a dimer of monohydride, as depicted in the model of figure 7c. On rare occasions we have also observed a feature labeled as "NRPH" in fig. 7b; this feature has an oblong shape reminiscent of the non-rotated "NRMH" and "NRD" dimers, but is asymmetric; we believe this feature could be attributed to a non-rotated dimer with only one H atom bonded to it, thereby having the structure DB-Si-Si-H(ads) (where DB= "dangling bond") and representing an intermediate between the NRMH and NRD structures for non-rotated dimers. Fig. 7c shows our assignments of the adsorbed species observed in fig. 7b. Note that because the SiH_2 groups and the NRMH structures break the dimer mirror-plane symmetry, they additionally induce dimer buckling which is not depicted in fig. 7c.

In addition to the small dimer structures discussed above, in this temperature range we also find that there are still some SiH_2 species present on the surface. In most cases, these SiH_2 groups appear on adjacent dimer rows, immediately next to one another. Such groups are labeled "P" in fig. 8a. In all respects, the appearance of these features as a function of bias voltage mirrors that of individual SiH_2 groups. For example, at negative sample bias individual SiH_2 groups show a characteristic depression around the central protrusion, (as in fig. 2b, 4b and 4c) which is also observed for the features labeled "P". Finally, quantitative analysis of the height changes (under constant-current conditions) reveals that the height change observed at the "P" features is identical to that observed over SiH_2 groups within the accuracy of the measurement (±0.1Å), as shown in fig. 8b. Based on the similarity between the features denoted "P" and those observed for individual SiH_2 groups, we assign the features shown in fig. 8a to pairs of SiH_2 groups in

which the two SiH_2 groups, each of which is bridge-bonded between two dimers within a single dimer row, are located on adjacent dimer rows.

As will be discussed later, the observation of the "non-rotated" clean dimer "NRD" , monohydride dimer "NRMH", dimer with one hydrogen "NRPH" and apparently paired SiH_2 groups ("P") provides important clues into the kinetics of the CVD dissociation mechanism.

Section III: Local structure and ordering of H atoms

The geometric and electronic properties of the clean Si(001) surface and of the Si(001)-(2x1)H monohydride surface and how these properties are manifested in STM images were delineated by Hamers, et al.[55, 56, 67-69]. For covalently-bonded systems, a molecular orbital approach can be used quite successfully to qualitatively understand the changes in electronic structure arising from dimerization and from adsorption of simple atomic species. Figure 9 shows a simplified energy diagram for two silicon atoms of the bulk-truncated surface before (a) and after (b) dimerization, while (c) and (d) depict the changes in electronic structure produced by adsorption of one or two hydrogen atoms, respectively; structure (d) is referred to as the Si(001)-(2x1)H monohydride structure.

At the bulk-truncated Si(001) surface, each surface Si atom has two sigma bonds to the bulk substrate (labeled "σ_S") and two half-filled, sp^3-hybridized dangling bonds (labeled "sp^3"). As originally noted by Appelbaum and co-workers[57] , the formation of a dimer can be understood as a rehybridization of these four sp^3-hybridized "dangling bonds" into molecular orbitals of the dimer which can be described as σ, π, σ^* and π^* in nature. The σ bond is quite strong but the π bond is weak, with the result that the splitting between the occupied π state and the unoccupied π^* state is small, less than 1 eV. As noted earlier, in STM images at negative sample bias electrons must tunnel out of occupied states of the sample, so that the STM images primarily reflect the spatial distribution of the occupied π state (lying 0.6 eV below E_F), while images at positive sample bias reflect the spatial distribution of the unoccupied π^* antibonding state (lying about 0.2 eV above E_F). Appelbaum, et al.[57, 70-72] mapped out the shape of the π and π^* orbitals at particular points in the surface Brillouin zone in a more elaborate model taking into account

the dispersion of the surface states due to the periodic nature of the surface. As expected, the π orbital is essentially bean-shaped, although the calculations predict a distinctly increased density of occupied states directly above the individual Si atoms for distances within a few Å of the dimer. Because the STM tip is about 8-10 Å from the dimers, however, STM images typically show only a bean-shaped structure with a maximum at the center of the Si=Si bond. Since the π^* orbital has a node at the center of the Si=Si dimer bond, the state density there drops to zero and the tip must push toward the sample to achieve constant tunneling current. The net result is that at positive sample bias, STM images show a pronounced splitting of the dimers, giving them the appearance of well-resolved atoms, as in fig. 2a. For the Si=Si dimers, then, there is a clear change in the spatial symmetry between negative and positive bias.

Adsorption of a single H atom on a Si=Si dimer breaks the π bond (leaving the strong σ-bond intact), and the sp^3 hybrid of one of the silicon atoms interacts with the 1s orbital of the hydrogen atom to form a Si-H bond, with associated σ_{Si-H} bonding and σ^*_{Si-H} antibonding states. Because the Si-H bond is strong, the σ_{Si-H} and σ^*_{Si-H} states will lie far away from each other, presumably far from the Fermi energy[71]. The other Si atom of the dimer is left with a half-filled sp^3-hybridized "dangling bond" which, because it is only partially occupied (nominally half-filled), it must lie at the Fermi energy. In STM experiments at moderate bias voltages, then, tunneling both in to and out of the "dangling bond" is quite facile, making the dangling bond appear as a protrusion. In contrast, the Si atom which is bonded to the hydrogen atom has decreased state density near E_F, so it appears as a dark depression. Thus, the STM essentially images the "dangling bond", and the actual H atom masks itself in such a way that it appears to be a vacancy. Because the adsorption of a single H atom onto a Si=Si dimer breaks the mirror plane which bisects the double bond of the Si=Si dimer, another effect of H adsorption is to induce tilting, or "buckling" of the dimer. As noted previously[51], dimer buckling can extend for tens of Angstroms away from such a site and can also extend to other dimer rows; this has the effect of making a surface with even a few adsorbed H atoms appear to be comparatively disordered and in some cases makes the interpretation of the data more difficult.

Adsorption of a second hydrogen atom onto a dimer produces the H-Si-Si-H "monohydride" structure. As depicted in fig. 9d, this can again be understood as a breaking of the weak π bond and the formation of strong σ_{Si-H} bonding and σ^*_{Si-H} antibonding orbitals which lie farther from E_F than the corresponding π and π^* orbitals of the clean Si=Si dimers. Indeed, Hamers, et al. showed that the energy of the Si-H antibonding states is approximately 1.5 eV above E_F and so could only be accessed by tunneling at comparatively high voltages, while the energy of the Si-H bonding state is very low in energy and not readily accessible to an STM experiment (tunneling at negative bias on this surface presumably takes place through bulk states or by hybridization of the Si-H bonding states with the bulk valence band). A comparison of 9b and 9d shows that the density of both occupied and unoccupied states near E_F is considerably higher for dimers of the "clean" surface than for the "monohydride". Based on these electronic structure considerations, dimers of the Si(001)-(2x1)H monohydride structure can be distinguished from "clean" Si=Si dimers in two ways: First, because of the increased state density near E_F, "clean" dimers are expected to appear higher than those of the monohydride structure. This fact has been verified by Boland [50, 63] for H-dosed Si(001) surfaces with positive sample bias. Secondly, the spatial distribution of tunneling current within the unit cell is different for dimers of "clean" and "monohydride" structures. This difference arises because STM images of the clean Si=Si dimers (probing the filled π-bonding state) show a maximum at the center of the Si=Si dimer bond, while images of the monohydride structure show higher state density at the ends of the dimers and a secondary minimum at the center of the H-Si-Si-H dimer, as will be seen later. The appearance of this secondary minimum is only observed with very sharp and symmetric tips, leading some[45] to question its existence. We find that tips which are able to easily resolve the dimers along a given dimer row of the clean surface also reproducibly show this minimum for dimers of the monohydride structure. The failure of some researchers to observe this minimum can likely be attributed to asymmetric or dull tips, or a high noise level which might mask its appearance. We further note that when imaging unoccupied states, both clean- and monohydride structures show maxima near the positions of the Si atoms, and so distinguishing between the structures must be done on the basis of the changed electronic state density rather than the detailed spatial distribution of this density.

The analysis described above serves as the basis for the ability to distinguish among various hydrogen-related structures and to tell whether the anisotropic islands consist of pure Si=Si dimers or dimers of the monohydride H-Si-Si-H. Figure 10a shows a Si(001) surface in the vicinity of a monatomic step which has been exposed to 0.6 Langmuir Si_2H_6 and then annealed to 660 K. On both terraces of the substrate, there are large dark areas which are anisotropic, extending further parallel to the dimer rows than perpendicular. Although it might be thought at first that these dark areas are vacancies, suitable adjusting of the contrast shows that they are not. Instead, with suitable contrast adjustment one finds that within these darker areas one can still clearly see dimers but each dimer shows two clear maxima separated by a weak minimum, just as expected for the Si(001)-(2x1)H monohydride. Because the difference in apparent height between the "clean" and monohydride structures is close to the 1.36 Å step height of Si(001), care must be taken to distinguish dimers of monohydride from vacancies. Here, the fact that the monohydride shows a clear dimer structure with differing spatial symmetry from the clean dimers serves as particularly valuable information.

After detailed analysis of figure 10a, we have made a "chemical map" of the surface, as shown in figure 10b. Here, ovals indicate "clean" dimers, and circles represent hydrogen atoms. Three terraces are visible: the lowest is the large terrace at lower left, the middle terrace consists of the large area at upper right and a few small islands growing on the terrace at lower left, and the higher consists of the small epitaxial islands growing on top of the large terrace at upper right. Species on the lowest terrace are filled in black, those on the middle terrace are shaded, and those one the highest terrace are open. Areas which are completely open (predominantly near the step edge) are regions in which the chemical composition cannot be determined unambiguously. Several pieces of information can be obtained from this analysis. First, we see that dimers of monohydride tend to be segregated together, so that the surface has partially phase-segregated into regions of clean silicon and regions of pure monohydride. Secondly, we note that whereas the small islands of silicon have coalescent into strongly anisotropic, one-dimensional "dimer strings", at low coverages (where such one-

dimensional dimer strings cover only a small fraction of the surface) the regions of monohydride are comparatively isotropic.

Because of the large apparent height difference between the clean dimers and the monohydride dimers, it can be difficult to see the structure clearly in a single grayscale image of fixed contrast, particularly when small sample-tip bias voltages are used during imaging. However, as the bias voltage is increased, the apparent contrast between clean and monohydride phases becomes small, making it much easier to distinguish the phases and to discriminate between monohydride and vacancies. Fig. 11a shows a region of Si(001) after exposure to 0.6 Langmuirs disilane and annealing to 660 Kelvin, imaged with a sample bias of -3.0 Volts. As before, large dark regions are observed, although now the contrast is reduced to only 0.8 Å between clean and monohydride regions. Figure 11b shows an enlarged view of the rectangular region indicated in fig. 11a; the minimum at the center of the Si-Si bond can be clearly observed for the monohydride dimers, and this, in conjunction with the apparent height difference between them and the clean dimers, allows one to determine the chemical composition on a dimer-by-dimer basis. Fig. 11c shows the height changes observed across the region between the arrows shown in fig. 11a; for dimers within a single atomic plane, those consisting of H-Si-Si-H are approximately 0.8Å lower than those of Si=Si. Additionally, the height profile shows that the spatial distribution of tunneling current for the monohydride phase shows two well-resolved maxima at the locations of the Si-H bonds (for example, over the monohydride dimer at a lateral distance of 70 Å), while for the clean Si=Si dimers there is a single maximum at the center of the Si=Si bond; this results in grayscale images of the monohydride phase showing two well-resolved protrusions in each unit cell while the Si=Si dimers appear like bean-shaped ovals, as in fig. 11b.

To study how the contrast between clean and monohydride regions changes as a function of applied bias, the region shown in figure 11a was repetitively scanned over a range of bias voltages, and height profiles like that shown in fig. 11c were measured to determine the contrast. The results, shown in fig. 12, demonstrate that at most bias voltages between -1.5 and -2.5 V, which are commonly used in STM experiments on Si(001), the monohydride

appears to be more than 1 Å lower than the Si=Si dimers, and can even appear lower by more than the 1.36 Å step height of Si(001). The result of this "electronic contrast" is that regions of monohydride can easily be mistaken for surface vacancies. Indeed, Boland[45] has suggested that the number density of defects on monohydride surfaces prepared by dosing Si(001) with atomic hydrogen is much lower than the defect concentration of the starting surfaces; our results demonstrate that vacancy defects and the monohydride structure have nearly the same height, thereby making vacancies nearly "invisible" over the range of bias voltages typically used in STM. As a result, for bias voltages between -1.6 and -2.6 V the height difference alone cannot be used to identify the monohydride structure; either the spatial symmetry of tunneling current within the unit cell must be used as auxiliary information, or else bias voltages of 3.0 Volts or greater must be used to distinguish between monohydride and simple vacancies. The ability to make this distinction is particularly important because of the possibility of silicon etching through formation and desorption of SiH_X species at elevated temperatures[24], which would produce regions containing true vacancies.

The ability to identify small monohydride regions is particularly important in our studies, since we desire to understand the fate of the hydrogen produced by dissociation of the SiH_X species at low temperatures, where hydrogen atoms can diffuse only short distances and may not form large regions of the segregated monohydride. Indeed, our experiments show that many of the structures which appear as vacancies at low bias voltages are in fact small regions, sometimes consisting of only one or two dimers, of the monohydride phase; these can be easily distinguished from true dimer vacancies only at bias voltages approaching 3 volts. With the clear understanding of the initial adsorption step at the room temperature, the differences in appearance and symmetry of the Si=Si dimers and the H-Si-Si-H monohydride dimers, it is possible to understand the changes in surface chemical and geometric structure which accompany dissociation of the SiH_2 fragments and diffusion of H(ads) with different thermal treatments.

Section IV: Diffusion of hydrogen and silicon and the formation of ordered phases

With a clear understanding of how to identify the various structures present on the surface provided by the work presented up to this point, we now consider the role of diffusion of these surface species on the formation of the ordered phases. Theoretical studies of hydrogen diffusion on Si(001) predict that the diffusion is strongly anisotropic, with H atoms diffusing much more quickly parallel to the dimer rows than in the perpendicular direction[41, 73, 74]. Likewise, STM studies of silicon show that both diffusion and sticking coefficients are anisotropic on this surface, further complicating the formation of epitaxial islands[60, 62, 75, 76]. The temperature range between 430 K and 540 K involves several chemical transformations as well as the onset of appreciable diffusion of both H and Si. Figures 13a and 13b show the Si(001) surface after exposure to 0.2L Si_2H_6 and then annealing to 430 Kelvin for 5 minutes. Comparing these images with those obtained without annealing, as in figure 1b, 2a, and 3a-3f, shows that there is some thermal dissociation, but there are still SiH_2 groups present on the surface in the bridge-bonded position. In a few cases, we now observe bean-shaped structures on the tops of the dimer rows and across the tops of two adjacent dimers within a dimer row. As described in the previous section, these are Si=Si dimers in their normal orientation. Other images show non-rotated "NRD" dimers. At 430 Kelvin, the hydrogen atoms are not sufficiently mobile to form ordered monohydride except in rare instances and/or at higher surface coverage; instead, they appear like single-atom vacancies and induce buckling in the surrounding regions, making the surface appear somewhat disordered.

After annealing to 470 Kelvin, there are many different structures present on the surface due to more complete dissociation and surface diffusion of Si and H atoms. As shown in figure 14, STM images at first appear complicated, but a more detailed analysis shows that the overall structure consists almost entirely of structures which we have already identified: individual SiH_2 groups, single Si=Si dimers in the normal "A" and "T" configurations, single rotated dimers in the "NRD" configuration, hydrogen atoms present either individually or forming single dimers of monohydride, and small cluster of 2-3 Si=Si dimers, representing the formation of "dimer strings". Statistics from large scale images such as fig. 14 show that out of the single Si=Si(ads) dimers, 46%, 30% and 24% are at four-fold sites ("NRD"), atop sites("A") and trough sites ("T") respectively. A closer analysis shows that most

of the small dark regions in figure 14 are not vacancies, but are very small regions of ordered monohydride structure. An example of this is shown in figure 15, where high-resolution images with suitable contrast adjustments show that these "dark" regions contain dimers whose dimer axis is parallel to those on the main plane, but which show two well-resolved protrusions per dimer; as noted earlier, this appearance is characteristic of H-Si-Si-H monohydride dimers. The preference for H adatoms to adsorb on the same dimer, and therefore to form dimers of monohydride structure even at low hydrogen coverage, has been previously studied by Boland using STM; our results are consistent with his observations of hydrogen pairing[49, 77].

After annealing to 505 K for 5 minutes, figures 16 and fig. 17 show that there is a further reduction in the number of SiH_2 groups. The primary surface species are dimers or small dimer strings of Si=Si dimers, and the formation of the monohydride structure can again be observed, now showing a smaller number of larger regions of the monohydride structure.

As noted earlier, the appearance of many molecular fragments is strongly bias dependent. Additionally, species which break the symmetry of the surface can induce dimers in adjacent regions to buckle, leading to zig-zag structures which propagate away from the adsorbates. In the temperature range of 430-540 K where there are many surface species present, the presence of dimer buckling tends to make the surface look very disordered because the buckling has a spatial extent comparable to the distance between adsorbates but has no well-defined long-range phase. As the applied bias is increased, we find that the dimer buckling appears less pronounced, making the surface appear more ordered and making it easier to distinguish adsorbates, monohydride, and vacancies. For example, figures 17a and 17b show a single region of the Si(001) surface exposed to 0.2 Langmuir disilane and then annealed to 505 Kelvin for 5 minutes, and imaged at a sample bias of -1.5 V (17a) and -2.5 V (17b). The central region of fig. 17a appears to be particularly disordered, due to the pronounced buckling of the dimers without any long-range order to the buckling direction. When imaged at higher bias (17b), however, the same area appears more ordered, and it becomes simple to identify the bonding position of the adsorbed species. At higher bias voltages, the measured corrugation between dimers is reduced; in order to see the

individual dimers the grayscale contrast must be higher, thereby making the adsorbed Si=Si dimers and other molecular fragments appear both higher and larger. Nevertheless, at the higher voltage one can clearly show that many "disordered" regions appear to consist of Si=Si dimers; also, as noted earlier, identifying the monohydride structure is easier at applied voltages near -3 Volts.

The decrease in the apparent magnitude of dimer buckling, and the concurrent improvement in the apparent degree of surface ordering which is observed as the bias voltage is increased can be understood in terms of the dimer electronic structure. It is widely recognized that dimer buckling is associated with a change in the dimer electronic structure, increasing the density of occupied states on the "up" atom, increasing the density of unoccupied states on the "down" atom, and increasing the energy separation between the occupied π state and the unoccupied π^* states[78]. In an STM experiment, the number of electronic states accessible to the tunneling process increases as the bias voltage is increased in magnitude. Consequently, STM images taken at low applied voltages would be expected to be more strongly affected by small changes in the surface electronic structure, while STM images at higher voltage will be less affected. We believe that the reason Si(001) surface looks more ordered at higher voltages (fig. 17b) and more disordered at lower voltages (fig. 17a) can be attributed to small local changes in the dimer electronic structure due either to dimer buckling or to interactions with nearby adsorbates, which then have a larger effect on STM images at low bias than at high bias. These images again point out the importance of understanding the surface electronic structure and the relation between the surface electronic structure and the STM images, in properly interpreting STM data on these complicated systems.

Annealing at higher temperature leads to further increases in the size of the epitaxial Si islands and better ordering of the regions of monohydride. For example, fig. 18 shows a Si(001) surface dosed with 0.2 L Si_2H_6 and then annealed at 540 Kelvin for 5 minutes. At this temperature, no SiH_2 groups are observed, and the silicon has primarily nucleated into dimer strings which are longer (2-5 dimers) and farther apart. Analysis of the images shows that the dimers in these dimer strings have only a single maximum instead of the two

maxima observed for monohydride dimers, and calibrated height profiles show that the height of these islands (1.4±0.1 Å higher than the underlying terrace) is nearly equal to the 1.36 Å step height on Si(001), indicating that they are "clean" Si=Si dimers. In contrast, if the islands were the monohydride phase, then based on the data in fig. 12 we would expect them to appear only 0.2 Å higher than the substrate terrace. (As well be discussed below, samples annealed at higher coverage and/or temperature do show the monohydride phase, demonstrating that our method for identification of these species is valid for the small epitaxial islands as well as extended terraces.) Thus, the islands formed by annealing the disilane-dosed surface to 540 K consist of primarily *clean* Si=Si dimers. Many of the small vacancies visible in the underlying terrace show the expected height and detailed spatial distribution characteristic of the monohydride structure, indicating that most of the hydrogen atoms are on the substrate terrace. Our results in this temperature regime indicate that the distribution of hydrogen between the dimer strings and the underlying substrate is non-statistical, with the hydrogen concentration (not just the total amount of adsorbed hydrogen) higher on the substrate than on the islands. Moreover, this non-statistical distribution is *opposite* to that reported in two brief previous studies[15, 16]. In the following section, we will show that at low temperatures and low coverage, the H atoms are found almost entirely on the flat terraces and only rarely on small epitaxial structures. At higher temperatures and/or higher coverages, the distribution of hydrogen between epitaxial islands becomes more nearly random, but hydrogen never shows a non-statistical preference for binding on epitaxial islands. The discrepancy between our work and the previous work [15, 16] has important implications for understanding the overall mechanism of the CVD process.

As the annealing temperature is increased, the islands begin to coalesce into longer dimer strings and small islands with a width of 2-3 dimers, as shown in fig. 19. At this annealing temperature, the monohydride structure is occasionally observed on the islands as well, indicating a more statistical distribution of hydrogen between substrate and islands. An example of a monohydride structure on an epitaxial island is indicated by the arrow in fig. 20a, and this region is enlarged in fig. 20b. As expected, the monohydride dimer on the epitaxial island shows a splitting and appears lower than the

"clean" dimers of the same terrace level, entirely consistent with our previous results and analysis. At the bias voltage of -1.8 V used for fig. 20, the Si(001)-(2x1)H structure is not easily distinguished from surface vacancies on the terrace. However detailed analysis of the images with different contrast adjustments and other STM images at different bias voltages shows that the substrate still contains some regions of monohydride, indicating that there remains a substantial amount of hydrogen on the surface.

The distribution of hydrogen between terrace and islands is also non-statistical at higher coverages. Figure 21 shows a large-scale (21a) and small-scale, high-resolution (21b) images of the Si(001) surface dosed with 0.6 Langmuir disilane and subsequently annealed to 630 Kelvin for 5 minutes. At this higher coverage the anisotropic growth of the silicon dimer strings can be observed more clearly. In fig. 21b, the STM tip was slightly asymmetric, such that the splitting of the monohydride is not easily observable. However, the monohydride dimers can still be recognized by their oblong shape and appearance approx. 1.3 Å lower than the other epitaxial dimers. For clarity, some regions of Si=Si epitaxial dimers are labeled "SED", and some regions of monohydride epitaxial dimers are labeled "MHED" in this figure. Figure 22a shows another large-scale image of a Si(001) surface including a step which has been exposed to 0.6 L Si_2H_6 and then annealed to 660 Kelvin. In this image, the splitting of the monohydride dimers on both terraces and on the epitaxial dimers makes their identification somewhat easier. Fig. 22b shows an enlarged view of one epitaxial island which includes monohydride structure in the middle of the string. Again, regions of Si=Si epitaxial dimers and monohydride epitaxial dimers are labeled "SED" and "MHED", respectively.

By direct counting of monohydride and "clean" silicon dimer units in a number of images at various temperatures, we have established that the distribution of hydrogen is clearly non-statistical at low temperatures. Detailed counting statistics were obtained on three different 250 Å x 250 Å regions of a sample annealed to 630 Kelvin; these statistics show under conditions where 35% of the substrate is H-covered, only 17% of the island area is H-covered; thus, hydrogen atoms are twice as likely to be found on terrace atoms as on substrate atoms. As the temperature is increased, this

anisotropy decreases. At 660 K, for example, when 44% of the substrate area is H-covered, 34% of the epitaxial island area is H-covered, indicating only a small preference for H atoms to bond on flat terraces. Particularly at the lower temperatures, a close inspection of the distribution of hydrogen on the epitaxial islands shows another interesting result: the distribution of hydrogen *within* a given epitaxial dimer string is not random; rather, the hydrogen atoms are preferentially observed in the central portions of a dimer string and are observed at the end of a dimer string only when the surrounding terrace has a high hydrogen concentration. This can also be observed from an analysis of figures 10, 11, 21 and 22.

Finally, figure 23 shows the surface exposed to 0.6 Langmuir Si_2H_6 and then annealed to 700 Kelvin for 5 minutes. At this annealing temperature, most of the hydrogen has desorbed from the surface, although small amounts can still be detected in high-resolution images. The Si has nucleated into larger islands than those observed at lower temperatures, and few one-dimensional "dimer strings" remain. The islands show the characteristic anisotropic shape previously noted in MBE studies[60], with an aspect ratio of between 2:1 and 3:1 for most islands. The initial nucleation of these islands on the substrate is apparently random. As these islands grow larger and intersect with each other or with existing step edges, there is a 50% probability that the "phase" of the (2x1) reconstruction of the intersecting islands will not match, resulting in the formation of two possible kinds of antiphase boundaries. Small regions of these antiphase boundaries are shown in fig. 23 and labeled "AP1" and "AP2". The AP2 boundaries cut across the dimer rows and form when the rows of the two islands meet with a lateral shift of 3.84 Å, while AP1 boundaries form parallel to the dimer rows of the islands and appear as a narrow row of vacancies. High-resolution images of AP2 boundaries show that they have a complicated structure extending over approximately 5 dimers; images of AP1 and AP2 boundaries produced by CVD are the same as those produced by MBE techniques and treated in more detail by Hamers, et al.[60, 75]. In a previous paper[79], we have shown that AP2 antiphase boundaries serve as preferential nucleation sites for epitaxial growth. Because this subject has been treated in more detail there, it will not be discussed further here.

DISCUSSION

1. Surface composition and surface reaction mechanism

Our STM images clearly reveal that over a rather wide temperature range, the surface contains a number of adsorbed species. Because the dissociation of the SiH_X species produces products which can occupy more surface sites than the reactants, it is reasonable to assume that more than one mechanism might be important in the overall decomposition of disilane on Si(001), depending on the coverage and temperature. Nevertheless, our STM images provide some important insight which allow us to rule out certain steps and suggest at least one primary mechanism for the overall reaction under the conditions used here.

Previous workers have studied the interaction of disilane, silane, and hydrogen with the Si(001) surface with a number of experimental techniques. In particular, temperature programmed desorption studies are particularly useful and complementary to our studies by providing information on the hydrogen desorption process. Additionally, because both the TPD experiments and our STM experiments are usually performed by dosing a low-temperature sample and then annealing, the experimental procedures are sufficiently close to permit a direct comparison.

Because hydrogen desorption ultimately plays an important role in the dissociation process, we consider it first. It is well-known[46, 47] that desorption of H_2 from H-saturated Si(001) surfaces occurs in at least two stages, although the temperatures at which these maxima occur differ among the various publications. The high-temperature desorption peak is referred to as the β_1 state and has its maximum at approximately 795 K; another peak, referred to as the β_2 state, occurs near 680K. It is generally accepted that the high-temperature β_1 state is due to H_2 desorption from the Si(001)-(2x1)H monohydride structure. Those studies[46, 47] have shown that this desorption is first order in coverage rather than the anticipated second order, leading to a considerable amount of speculation as to the detailed mechanism of the desorption process. It is generally believed that the β_2 state arises from the desorption of H_2 from higher hydrides such as SiH_2 and SiH_3; the kinetics of the β_2 desorption has not been as well studied, but investigations using isothermal decomposition and infrared spectroscopy [44] and using

temperature-programmed secondary-ion mass spectroscopy [28, 80] indicate that the β_2 peak is second-order.

TPD studies by Gates, et al.[26, 27] for silane on Si(001) and by Bozso, et al.[35] for disilane on Si(001) show two main features which are nearly identical to those observed for the hydrogen-dosed surfaces, suggesting that the desorption of hydrogen from SiH_X molecular fragments is not significantly different from that of SiH_X species on extended terraces. For Si(001) dosed with disilane, Bozso, et al.[35] also observed an additional broad desorption feature extending below 450 K, placing it 100 Kelvin below his temperature for the β_2 peak. Based on these combined results from a number of experimental techniques, the following set of possible reactions for disilane dissociation can be suggested:

For the room temperature (RT) initial adsorption, we can have:

$Si_2H_6(g) \rightarrow Si_2H_6(p)$	(at RT)	(i)
$Si_2H_6(p) \rightarrow 2SiH_3(ads)$	(RT)	(ii)
$SiH_3(ads) \rightarrow SiH_2(ads) + H(ads)$	(RT)	(iii)

After the disilane-dosed sample is annealed, the following reactions could take place:

$2SiH_2(ads) \rightarrow H_2(g) + H\text{-}Si\text{-}Si\text{-}H(ads)$	(iv-a)
$SiH_2(ads) \rightarrow H(ads) + SiH(ads)$	(iv-b)
$2SiH_2(ads) \rightarrow 2H(ads) + H\text{-}Si\text{-}Si\text{-}H\ (ads)$	(iv-c)
$SiH_2(ads) \rightarrow H_2(g) + Si(ads)$	(iv-d)
$H\text{-}Si\text{-}Si\text{-}H(ads) \rightarrow Si{=}Si(ads) + 2H(ads)$	(v-a)
$H\text{-}Si\text{-}Si\text{-}H(ads) \rightarrow Si{=}Si(ads) + H_2(g)$	(v-b)
$H(ads) + H(ads) \rightarrow H_2(g)$	(vi)

where the subscripts p, ads, and g refer to physisorbed, adsorbed (chemisorbed), and gas-phase states, respectively.

In an earlier report[51], we discussed the room-temperature processes involved in (i), (ii) and (iii). Our ability to observe SiH_3 groups and also to

observe their dissociation, as in figures 3-4, indicates that SiH_3 groups are stable enough to image in the STM (time scale of seconds), but dissociate on a measurable time scale on the order of minutes. Through direct counting of the number of adsorbed H atoms and adsorbed SiH_2 groups visible in the STM images, we find that the ratio of H(ads) to SiH_2(ads) is nearly 1:1. This surface stoichiometry demonstrates that reactions (i),(ii), and (iii) above likely the primary steps in the initial adsorption and shows that alternative steps for the initial adsorption, such as $Si_2H_6 \rightarrow SiH_2(ads) + SiH_4(gas)$, do not play an important role. The same conclusion has been reached in other studies of this system using static secondary-ion mass spectroscopy (SSIMS)[26].

The stability of SiH_3 groups on the Si(001) and the Si(111)-(7x7) surface has been controversial[26, 81, 82] and appears to depend on a number of factors. Because hydrogen produced by thermal decomposition blocks available surface sites, the thermal stability of all SiH_x species is quite sensitive to the local hydrogen coverage. Additionally, Gates, et al. found that SiH_3 groups produced by disilane adsorption appeared to be more stable than those produced by silane, even though these two precursors lead to nearly the same surface hydrogen coverage. At low coverage, where H atoms do not block available surface sites, they found that SiH_3 groups were quite unstable and dissociated with an activation barrier of only 2 kcal/mol when starting with SiH_4, but with a barrier of 6.3 kcal/mole and a prefactor of 50 s^{-1} when starting with Si_2H_6[26]. Lubben, et al.[37] also obtained a value of 13.1±3.5 kcal/mole and a prefactor of $2x10^5$ s^{-1} at low coverage.

Our results are in good agreement with the results of Gates and co-workers in that we also find that SiH_3 groups are unstable at room temperature, spontaneously dissociating via the reaction $SiH_3(ads) \rightarrow SiH_2(ads)$ + H(ads). The activation barriers and prefactors measured by Gates[26] and by Ludden[37] for the dissociation of SiH_3 groups produced from Si_2H_6 are both consistent with our results, which show that SiH_3 groups adsorbed on flat terraces without any nearby adsorbates dissociate on the time scale of a few minutes. However, the activation barrier for SiH_3 dissociation of only 2 kcal/mole obtained by Gates for dissociation of SiH_3 groups using SiH_4 as a precursor is too small to be consistent with our data. We believe that this might be explained in terms of defect chemistry. While our experiments have

shown that disilane adsorbs homogeneously on the surface, previous studies have suggested that this is not the case for silane, which is believed to adsorb preferentially at defect sites[26]. If SiH_3 groups at these defect sites dissociate more readily than those on more perfect surfaces, it would explain why SiH_3 groups from silane behave differently than those from disilane. Furthermore, it might explain the unusually low activation barrier of 2 kcal/mole obtained by Gates, et al. for SiH_3 dissociation at low coverage from the adsorption of SiH_4. Because the defect concentration on the Si(001) surface is typically at least a few percent[55], studies of SiH_3 dissociation kinetics at low coverage using area-averaging surface science techniques might be dominated by activity at these defect sites, leading to anomalously low activation barriers compared with what we observe away from defects.

Further decomposition of the SiH_2 groups might take place in a number of ways, given by reactions iv-a through iv-d. One of the primary questions in the further dissociation is whether SiH(ads) exists as a distinct, stable intermediate between SiH_2(ads) and Si(ads). From a chemical standpoint, it is easy to see how SiH_3 groups and SiH_2 groups form stable intermediates in the decomposition, since in both cases the adsorbed fragment can achieve four-fold coordination by simply breaking the weak π-bonds of one or two surface dimers, respectively. However, it is considerably more difficult to predict how an SiH group might bond to the surface in such a way as to achieve overall four-fold coordination, since this requires forming three new bonds to the surface in a nearly-tetrahedral geometry.

The temperature-programmed desorption (TPD) studies provide important information for understanding this reaction. Since an ordered Si(001)-(2x1)H monohydride structure, in which each surface silicon atom is bonded to one hydrogen atom, occurs at temperature between the β_1 and β_2 desorption peaks[40, 46, 47], we can conclude that the β_1 peak must arise from desorption from the monohydride phase. Then, it can be concluded that the β_2 peak observed in TPD must arise from species in which more than one hydrogen atom is bonded to a single silicon atom. It is difficult to explain the presence of the β_2 peak without invoking either direct desorption of molecular hydrogen from a SiH_2 or SiH_3 group, or a bimolecular reaction between adsorbed surface species to liberate molecular H_2.

The TPD experiments, in conjunction with our experiments, rule out direct desorption from either SiH_2 or SiH_3 groups as the origin of the β_2 peak. As noted above, decomposition of SiH_3 to SiH_2 occurs at room temperature, producing equal amounts of SiH_2(ads) and H(ads). If dissociation of SiH_2 occurred primarily by the reaction $SiH_2(ads) \rightarrow H_2(g)+Si(ads)$, then one atom of surface hydrogen (contributing to the β_1 peak) would be produced for each SiH_3 which dissociates, but two atoms would be produced for each SiH_2 which dissociated. As a result, the area under the β_2 peak would have an area twice that of the β_1 peak. This is clearly in disagreement with experiments by Isobe, et al.[83] using Si_2H_6/Si(001) and Gates, et al.[26] using SiH4/Si(001), who both found that the β_2 peak for H_2 desorption has an area only about *half* that of the β_1 peak. A similar height ratio is observed in desorption of H_2 from the hydrogen-saturated Si(001)-(2x1) surface (produced by exposure to atomic hydrogen), in which the β_2 peak presumably arises from interaction of SiH_2 groups in the surface plane rather than between adsorbed SiH_2 groups[47, 84]. One important conclusion which can be drawn from the TPD experiments, then, is that decomposition of SiH_2 must produce substantial amounts of hydrogen adsorbed on the surface. As a result, process (iv-d) should be ruled out as the major channel for the initial decomposition of SiH_2(ads) at low and intermediate coverages.

Of the remaining processes (iv-a) through (iv-c), reaction (iv-b) presumes the existence of an adsorbed SiH(ads) group, while reactions (iv-a) and (iv-c) are bimolecular. Despite the fact that bimolecular reactions usually have a low probability at low coverage, our STM images argue in favor of a bimolecular reaction as the primary SiH_2 dissociation step and argue against the successive release of hydrogen atoms to the surface from SiH_2 through the formation of a stable SiH intermediate.

Three observations argue against reaction (iv-b). First, we note that in our STM images, all the species can be identified as SiH_3(ads), SiH_2(ads), H(ads), or one of the dimer complexes; there are no "characteristic features" that we might be able to assign to an SiH(ads) group. However, it is possible that if SiH was a short-lived intermediate it might not be observed until after further dissociation to Si and H. Secondly, we note that reaction (iv-b) does not explain

the presence of β_2 desorption peak in TPD; since hydrogen desorbs molecularly, the sequential decomposition of SiH_2 through the reaction $SiH_3(ads) \rightarrow H(ads) + SiH_2(ads)$ followed by $SiH(ads) \rightarrow Si(ads) + H(ads)$ should produce two atoms of surface-adsorbed hydrogen which are identical to those produced by the initial SiH_3 dissociation; i.e., this reaction sequence fails to predict *any* β_2 peak. Also, we note that our STM images in the temperature range where the SiH_x species have dissociated but hydrogen has not yet desorbed from the monohydride phase show that the surface hydrogen-to-silicon ratio is close to 2:1, whereas the reaction sequence in (iv-b) would predict that the ratio of adsorbed H atoms to adsorbed Si atoms (from Si_2H_6 decomposition) would be 3:1. Based on the STM and previous TPD results, we believe that reaction (iv-b) can be eliminated as the primary SiH_2 dissociation pathway.

The elimination of processes (iv-d) and (iv-b) leaves only the bimolecular processes (iv-a) and (iv-c). Given the strong bond formed by two surface-adsorbed silicon atoms in the formation of a dimer, it is not surprising that pairing ultimately plays an important role in the chemistry on this surface. The images shown in figures 5, 7, 8, 14 and 15 clearly show the importance of pairing of silicon atoms into dimers, which occurs well before these dimers coagulate into larger islands. Our observation of "non-rotated" dimers, visible in figures 5, 7, 8, 14 and 15, in conjunction with our observation of features we attribute to non-rotated dimers which a hydride structure ("NRMH") strongly suggests that the pairing occurs through the bimolecular reaction $SiH_2 + SiH_2 \rightarrow$ H-Si-Si-H + $H_2(gas)$, followed by the step H-Si-Si-H $\rightarrow$ Si=Si + 2H(ads), where H-Si-Si-H is formed in the "NRMH" structure, and the Si=Si dimer formed as the product of the reaction is in the "NRD" geometry, which we observe frequently on the surface. Because this reaction sequence produces two atoms of surface-adsorbed hydrogen and only one atom of gas-phase (molecular) hydrogen from each SiH_3 group, it predicts that the β_1 peak should have twice the area of the β_2 peak, in agreement with the TPD result and our counting statistics. Likewise, it predicts a ratio of 2:1 for the ratio of surface hydrogen to epitaxial silicon, in agreement with our counting statistics. The alternative pairing reaction, given by (iv-c), would predict no β_2 and a larger surface hydrogen to silicon ratio, which we believe is inconsistent with both the STM and TPD results.

The possibility of such a pairing mechanism has been considered previously by Y. Suda, et al.[36] and J. J. Boland[16]. Suda, et al.[36] performed EELS and RHEED studies, while Boland performed scanning tunneling microscopy studies of the monohydride phase. Both proposed that SiH_2(ads) groups might be bonded atop dimers, and that the interaction between two such SiH_2 groups on adjacent dimers on the same dimer row could lead to the formation of a dimer in the configuration (b) shown in figure 6. Their mechanism is shown in fig. 24a. However, those studies were based on the incorrect assumption that the stable configuration for SiH_2(ads) consisted of an SiH_2 fragment bonded to the two silicon atoms of a single dimer, leading them to propose that two SiH_2 groups might approach along the dimer row direction ($[1\bar{1}0]$), reacting to form a dimer of monohydride which is in the normal direction for epitaxial growth. In contrast, our results show that the SiH_2 groups bond to two dimers within a single dimer row; as a result, the logical direction for approach would be perpendicular to the dimer rows, along the [110] direction. Figure 24b shows our proposed mechanism for SiH_2 decomposition on the Si(001) surface. We propose that the primary mechanism is that two SiH_2 groups diffuse on the surface until they are located immediately adjacent to one another on different dimer rows. This position puts two of the hydrogen atoms in close proximity, allowing them to combine into H_2(gas) with the concurrent formation of a sigma-bonded H-Si-Si-H group which we observe as the "NRMH" specie depicted in fig. 7. This specie is essentially a monohydride dimer, which can then lose further hydrogen either by surface diffusion or through desorption into the gas phase to form a dimer of "clean" silicon in the non-rotated geometry, which we observe as the "NRD" dimers in fig. 5. Finally, the non-rotated dimers can rotate into the normal epitaxial orientations to produce the "A" and "T" species also shown in fig. 5.

2. Hydrogen diffusion and monohydride formation

One of the primary differences between epitaxial growth via CVD techniques and via MBE techniques is the presence of surface hydrogen in the former but not in the latter. Due to the different binding energies for Si-H and Si-Si, it is reasonable to assume that surface hydrogen will affect not only the chemistry of the CVD process, but also will affect the physical processes of

nucleation, diffusion, and growth. The STM images in figure 10a, 11a, 11b, 21 and 22 show the possibility of hydrogen diffusion into an ordered (2x1)-H monohydride region on the terraces of the substrate and also the epitaxial islands. This preferential pairing of hydrogen atoms onto adjacent dimers was first noted by Boland[49] for atomic hydrogen interacting with the planar Si(001) surface. In order to provide insight into the fate of the hydrogen atoms produced by the decomposition of disilane, we have analyzed the spatial location of the hydrogen atoms on the terraces and on the islands as a function of temperature. If the silicon islands are formed by the diffusion of SiH monohydride units across the surface, then we would expect the probability of finding an H atoms on the island Si atoms to be higher than the probability of finding an H atom on the terrace Si atoms. Indeed, we find that the opposite is true at lower temperatures. Below 570K, we find little or no monohydride on the epitaxial islands, even though it is clearly visible on the substrate. As the temperature increases, we find that the fraction of the surface area covered by hydrogen for the substrate and the epitaxial islands approach the same value, but with the fractional coverage on the epitaxial islands always lower than that of the substrate. At 630 Kelvin, for example, images in which 35% of the substrate is H-covered show that only 17% of the island area is H-covered. At 660 K, in images where 44% of the substrate area is H-covered, only 34% of the epitaxial island area is H-covered. Indeed, even the individual dimers formed by annealing at low temperatures (as in fig. 5, 7, 8 and 14) are usually dimers of *clean* silicon. At higher temperatures, the spatial distribution becomes more uniform as diffusion and desorption of hydrogen both become rapid on the time scale of the annealing experiment. As noted earlier, a close examination of the distribution of hydrogen on the epitaxial islands also shows that the "monohydride" dimers are usually only observed near the center of the dimer strings, and are only observed at the ends of the dimer strings when the surrounding substrate region also consists of the monohydride phase. Thus, our images lead us to conclude that H atoms preferentially adsorb on the terraces at low temperatures, but as the temperature is increased, they diffuse sufficiently to randomize their distribution between islands and the substrate terrace.

This spatial distribution of H atoms could have several possible origins. One possible origin could be that H atoms are thermodynamically less stable on

the initial epitaxial islands than on the terrace. Such a difference in stability might result from slight differences in strain energy between narrow islands and extended terraces, since it is known that the Si(001) reconstruction involves substantial strains extending several layers into the terrace. Wu and Carter[73, 85] found that the difference in binding energies between two H atoms bonded on different dimers and on the same dimer (thereby forming a dimer of monohydride) was too small to account for the preferential pairing observed by Boland[49, 77] and proposed that long-range strain effects might be important. Alternatively, the differences in site occupancy might arise from the kinetics of hydrogen diffusion on and/or desorption from the surface vs. epitaxial islands. In the narrow epitaxial islands, a very large fraction of the atoms are essentially at step edges. In the initially-formed dimer "strings", all of the dimers are like those at type "A" step edges, while those at the ends are also like those at type "B" step edges. If the rate of desorption from a type "B" step edge is comparable to or larger than the rate of surface diffusion of hydrogen atoms to the step edge, then a "bare" region of the surface will be formed. Our observation of "bare" regions at the ends of epitaxial silicon islands (but with monohydride in the interior) might then be attributed to hydrogen atoms desorbing from the type "B" step edges faster than they can be replenished by surface diffusion.

Our experimental results indicate that dissociation of SiH_x species occurs completely to Si dimers and adsorbed H atoms before the adsorbed SiH_x species can coagulate into islands larger than a single dimer. This conclusion is important because it contradicts two previous studies[15, 16] of disilane adsorption/decomposition on Si(001) and has important implications for the overall reaction mechanism. In order to understand the arguments on both sides, it is important to understand the electronic structure of the clean Si(001) surface and the monohydride surface. As depicted in fig. 9, the reconstruction of a clean Si surface results in the formation of occupied π and unoccupied π^*-antibonding states as shown from fig. 9a to fig. 9b. Published results from various authors[55, 56] agree that clean Si dimers show a symmetric bean shape when imaged at negative sample bias, but are clearly split into two well resolved protrusions at positive bias due to the nodal structure of the π^*-antibonding state. The addition of hydrogen to form the monohydride structure sweeps the surface states out of the gap, producing occupied Si-H

bonding states which lie far below E_F, and producing an unoccupied Si-H state approximately 1.5 eV above E_F[67]. When imaged at positive bias, then, both the clean surface and the H-terminated surface show a characteristic splitting of the dimer structure, and "clean" dimers appear higher then "monohydride" dimers because the density of states associated with the dimer π-bond is larger than those of the Si-H antibonding states. At negative bias (imaging occupied states), the experimental results seem contradictory. Hamers, et al.[67, 69] originally showed that dimers of the "monohydride" structure again show a splitting, due presumably to hybridization of the Si-H bonding states with the valence band. Likewise, Boland has shown this characteristic splitting in dimers of the H-Si-Si-H structure which arise as part of the Si(001)-(3x1)-H surface[77], in which monohydride H-Si-Si-H dimers alternate with SiH_2 groups to give an overall (3x1) periodicity. Indeed, this splitting is clearly shown in fig. 10, 11 and 22, which show occupied states of both clean- and H-terminated dimers on two terraces, thereby ruling out any artifacts that might be due, for example, to an asymmetric STM tip. The dimers of monohydride appear lower and show a splitting. However, in an STM image the presence or absence of internal structure within the unit cell depends critically on the sharpness of the STM tip. Dull tips, which may not even be able to resolve the individual dimers within a dimer row, certainly will not be able to resolve the shorter-range corrugations leading to the splitting of the empty states of the H-terminated dimers. Based on our ability to individually identify "clean" and "monohydride" dimers on two terraces simultaneously as shown in fig. 10 and 22, we believe that the failure of some experiments[15, 77] to see the splitting is most likely an indication of a dull or asymmetric tip.

The first STM study of disilane on Si(001) by Boland[16] reported the formation of islands, which he attributed to the monohydride structure. The assignment of these islands to the monohydride structure, however, was not based on any observations of the apparent height or appearance of "split" dimers; instead, it was made solely on the basis of tunneling spectroscopy measurements and the presence of an occupied state feature approximately 1.5 eV above E_F. We believe that the assignment of chemical identity based solely on the basis of the STS measurement, without an accompanying measurement on a "clean" dimer made with the same tip under identical conditions, is probably unreliable and is responsible for Boland's incorrect conclusion.

Even at comparatively high coverage, for example, with a good STM height calibrations, for example, we showed in our previous paper and here, in figure 10-13, that the epitaxial islands of clean Si appear higher than the substrate by almost exactly 1.36 Å, the step height on Si(001), while islands of monohydride appear only about 0.5 Å higher than clean dimers of the underlying terrace (i.e., epitaxial dimers appear nearly 1 Å lower than "clean" dimers in the same epitaxial layer). We find that this apparent height difference is the most reliable indicator of the chemical identity of any individual dimer, and the apparent splitting of the occupied-state images further evidence for monohydride formation. When imaging unoccupied states, however, both our studies and Boland's studies show that the dimers appear split, due to the characteristic node in the π^*-antibonding state for clean Si dimers, and due to tunneling into the well-separated Si-H antibonding states for the monohydride.

Lin, et al.[15] likewise attributed their islands to the monohydride structure based on images showing at positive sample bias (imaging unoccupied states) the dimer strings appeared to be split but those on the terrace were not, while corresponding negative-bias images (filled states) showed bean-shaped structures on both lower and upper terraces; In neither case could individual dimers be resolved. They concluded that their empty state images proved that the epitaxial dimer strings were monohydride because the epitaxial dimers appeared to be split. However, as noted above and as shown in figure 2, the appearance of a splitting when imaging the *empty* state does not prove monohydride formation, since as shown in figure 2, atomic resolution images of the empty states of clean Si(001) surface show a splitting as well. Furthermore, Lin's image of the occupied states show no splitting on either the substrate terrace and on the epitaxial islands; as shown in fig. 10, 11 and 22, however, occupied-state images of the clean surface should show bean-shaped structures, while occupied-state images of the monohydride phase show a splitting if the STM tip is sufficiently sharp. The observation of a splitting of the empty state images of the epitaxial dimers but not on the terrace could easily be attributed to an asymmetric tip, which permitted them to observe the (expected) splitting of clean dimers on the epitaxial terrace, but not on the substrate terrace; since they were unable to resolve dimers on either terrace, such an explanation seems quite likely.

Irrespective of the origin of this discrepancies with previous studies, we believe that our data, particularly the ability to resolve individual dimers of "clean" silicon and of the monohydride structure, conclusively demonstrates that the "dimer strings" formed by annealing disilane-dosed surfaces consist primarily of clean silicon dimers. This point is important because it provides strong evidence for the mechanism of the formation of epitaxial islands: SiH_2 groups pair, losing one molecule of H_2 to the gas phase and producing individual "non-rotated" monohydride dimers (NRMH). The adsorbed NRMH dimers then each lose 2 H atoms to the extended surface layer to form non-rotated dimers (NRD). Since we observe individual NRD dimers but never observe larger NRD islands, we presume that the individual NRD dimers dissociate into silicon atoms, when then diffuse and nucleate into the more common epitaxial Si=Si dimers atop a substrate which is partially hydrogen-covered. We observe no significant direct ordering of adsorbed SiH_x species except for the initial pairing for the NRMH dimers. Thus, the formation of extended islands of clean epitaxial silicon is due to the diffusion and nucleation of Si atoms on a partially H-covered surface, while extended regions of monohydride are formed by subsequent diffusion of H from the substrate onto the epitaxial islands.

From the images in fig. 14, 15, 21 and 22, we see that diffusion of hydrogen and its accumulation into "islands" occurs in the same temperature regime as diffusion of silicon atoms and the formation of dimer strings, but the silicon islands show more long-range order than do the regions of monohydride. Small regions of the monohydride phase form at temperatures as low as 470K, and we observe complete coagulation of hydrogen into the monohydride phase (and the disappearance of features attributed to individual adsorbed H atoms) at temperatures of 570 K and higher. Boland also observed the formation of the monohydride phase after exposing a Si(001) surface to hydrogen atoms and annealing to 690 Kelvin for 10 seconds. It is also interesting to note that in cases where the surface consists of partially "clean" Si=Si dimers and partially of the monohydride phase, the silicon dimer strings shown a greater degree of anisotropy than the monohydride regions, although the latter may show some small degree of anisotropy. As noted in previous STM studies of clean silicon surfaces, such anisotropy can have both

thermodynamic and kinetic factors. Because Si(001) step edges have a lower energy if the step edge is parallel to the dimer row than if it cuts across the dimer rows, islands of Si on Si(001) have some thermodynamic anisotropy. Additionally, kinetic factors such as the sticking coefficient for diffusing adatoms and the rate of surface diffusion can be anisotropic, resulting in kinetic anisotropies. In an analogous manner, the anisotropy of the monohydride regions can have both thermodynamic and kinetic influences which must be explored further.

3. A comparison of low-temperature CVD with MBE

Since chemical vapor deposition (CVD) and molecular beam epitaxy (MBE) represent competing techniques for the growth of silicon, a comparison between these two is warranted. The primary difference between the CVD process and the MBE process, particularly at low temperatures, is the presence of surface hydrogen in the former but not in the latter. At temperatures where the SiH_2 groups have dissociated, the primary species present on the surface are silicon dimers and adsorbed hydrogen atoms, which may or may not have segregated into a separate monohydride phase. The existence of H ad-atoms may play an important role in the CVD process by affecting the sticking of incident molecules or by limiting the diffusion of Si ad-atoms. A further observation of the effect of hydrogen as a diffusion-blocker can be drawn from a comparison of the average length and aspect ratio of the growing islands shown here with those presented in earlier studies under molecular-beam epitaxy (MBE) conditions. Those studies[60, 75, 86] showed that epitaxial growth at temperatures near 700 Kelvin produced long islands only one dimer wide, but with a length as long as 60 dimers, producing narrow dimer strings with an aspect ratio of 30:1. The length and aspect ratio of these dimer strings and larger two-dimensional islands is strongly temperature-dependent and can be time dependent, since the anisotropy has both kinetic and thermodynamic origins. As the temperature is increased or the annealing time lengthened, the island density becomes lower and the aspect ratio of the resulting larger islands becomes closer to unity, generally approaching between 2:1 and 3:1. Under similar CVD conditions (for example, see fig. 23, grown at 700 Kelvin), we typically find that the number density of islands is substantially higher, with most islands consisting of short dimer strings one dimer wide and only a few dimers long. The presence of large numbers of

small islands indicates that the diffusion is inhibited, which must be a result of the surface hydrogen. After annealing at temperatures above the hydrogen desorption temperature, the aspect ratio and overall shape of the islands much closely approaches that of the MBE experiments, with island aspect ratios of between 2:1 and 3:1 commonly observed. Our results are consistent with previous results by Lin, et al.[15], who showed that islands produced by disilane decomposition on Si(001) are smaller than those produced by solid-phase epitaxy under otherwise similar conditions. Clearly, a full understanding of the role of hydrogen as a diffusion inhibitor in CVD will require a more thorough analysis which will be carried out in the future. The STM images shown here, however, suffice to show at least qualitatively that hydrogen affects the surface growth kinetics by reducing the rate of surface diffusion and thereby stabilizing small islands on the surface.

CONCLUSIONS

Through a detailed study of the successive stages in the thermal decomposition of the molecule disilane on the Si(001) surface, we have identified the initial adsorbates and the key intermediates in the dissociation of disilane on Si(001) and the epitaxial growth of silicon islands on this surface. We have directly observed the adsorption of SiH_3 groups onto Si "dangling-bond" sites, and have directly observed their dissociation into SiH_2 groups and H atoms on the time scale of several minutes. Our experiments reveal the presence of several previously-unobserved features, including several "non-rotated" dimer species which we believe are key intermediates in the dissociation of SiH_2 groups. We find no evidence for a stable SiH intermediate, but find strong evidence for SiH_2 decomposition through a non-rotated monohydride dimer, when then loses hydrogen to form a non-rotated "clean" dimer and adsorbed H atoms. Using voltage-dependent STM imaging, we have also demonstrated the ability to distinguish on a dimer-by-dimer basis between dimers of "clean" Si and dimers of the monohydride structure. From these images, we are able to show that, contrary to previous experiments, the CVD process does not occur by coagulation of SiH_X species which then decompose, but by decomposition of the SiH_X species followed by nucleation and growth of the Si islands.

ACKNOWLEDGMENTS

This work was supported in part by the U.S. Office of Naval Research and the National Science Foundation. MJB would like to thank the National Science Foundation for an NSF Postdoctoral Research Fellowship in Chemistry

REFERENCES

[1] B. S. Meyerson, Proc. IEEE 80 (1992) 1592.

[2] B. S. Meyerson, Appl. Phys. Lett. 48 (1986) 797.

[3] J. Murota, M. Sakuraba and S. Ono, Appl. Phys. Lett. 62 (1993) 2253.

[4] E. Sirtl, L. P. Hunt and D. H. Sawyer, J. Electrochem. Soc. 121 (1974) 919.

[5] W. A. P. Claassen and J. Bloem, J. Crystal Growth 50 (1980) 807.

[6] D. D. Koleske, S. M. Gates and D. B. Beach, Appl. Phys. Lett. 61 (1992) 1802.

[7] T. Tatsumi, K. Aketagawa, M. Hiroi and J. Sakai, J. Crystal Growth 120 (1992) 275.

[8] S. M. Gates, Surf. Sci. 195 (1988) 307.

[9] J. M. Jasinski and S. M. Gates, Acct. Chem. Res. 24 (1991) 915.

[10] S. M. Gates, J. Phys. Chem. 96 (1992) 10439.

[11] S. M. Gates, D. D. Koleske, J. R. Heath and M. Copel, Appl. Phys. Lett. 62 (1993) 510.

[12] J. M. Jasinski, B. S. Meyerson and B. A. Scott, Ann. Rev. Phys. Chem. 38 (1987) 109.

[13] W. K. Liu, S. M. Mokler, N. Ohtani, C. Roberts and B. A. Joyce, Surf. Sci. 264 (1992) 301.

[14] S. M. Mokler, W. K. Liu, N. Ohtani and B. A. Joyce, J. Crystal Growth 120 (1992) 290.

[15] D. S. Lin, E. S. Hirschorn, T. C. Chiang, R. Tsu, D. Lubben and J. E. Greene, Phys. Rev. B 45 (1992) 3494.

[16] J. J. Boland, Phys. Rev. B 44 (1991) 1383.

[17] H. Hirayama, M. Hiroi, K. Koyama and T. Tatsumi, Appl. Phys. Lett. 56 (1990) 1107.

[18] M. Hiroi and T. Tatsumi, J. Crystal Growth 120 (1992) 279.

[19] D. S. Mui, S. F. Fang and H. Morkoc, Appl. Phys. Lett. 59 (1991) 1887.

[20] S. M. Mokler, N. Ohtani, J. Zhang and B. A. Joyce, Surf. Sci. 275 (1992) 401.

[21] S. M. Mokler, W. K. Liu, N. Ohtani, J. Zhang and B. A. Joyce, Surf. Sci. 275 (1992) 16.

[22] S. M. Mokler, W. K. Liu, N. Ohtani and B. A. Joyce, J. Vac. Sci. Technol. A 10 (1992) 1846.

[23] S. M. Gates, B. A. Scott, D. B. Beach, R. Imbihl and J. E. Demuth, J. Vac. Sci. Technol. A 5 (1987) 628.

[24] S. M. Gates, R. R. Kunz and C. M. Greenlief, Surf. Sci. 207 (1989) 364.

[25] S. M. Gates, C. M. Greenlief, D. B. Beach and R. R. Kunz, Chem. Phys. Lett. 154 (1989) 505.

[26] S. M. Gates, C. M. Greenlief and D. B. Beach, J. Chem. Phys. 93 (1990) 7493.

[27] S. M. Gates, C. M. Greenlief, D. B. Beach and P. A. Holbert, J. Chem. Phys. 92 (1990) 3144.

[28] S. M. Gates, C. M. Greenlief, S. K. Kulkarni and H. H. Sawin, J. Vac. Sci. Technol. A 8 (1990) 2965.

[29] S. M. Gates and C. M. Chiang, Chem. Phys. Lett. 184 (1991) 448.

[30] S. M. Gates and S. K. Kulkarni, Appl. Phys. Lett. 58 (1991) 2963.

[31] S. M. Gates and D. D. Koleske, Appl. Phys. Lett. 61 (1992) 309.

[32] S. M. Gates, C. M. Chiang and D. B. Beach, J. Appl. Phys. 72 (1992) 246.

[33] S. M. Gates, J. Crystal Growth 120 (1992) 269.

[34] S. M. Gates and S. K. Kulkarni, Appl. Phys. Lett. 60 (1992) 53.

[35] F. Bozso and P. Avouris, Phys. Rev. B 43 (1991) 1847.

[36] Y. Suda, D. Lubben, T. Motooka and J. E. Greene, J. Vac. Sci. Technol. A 8 (1990) 61.

[37] D. Lubben, R. Tsu, T. R. Bramblett and J. E. Greene, J. Vac. Sci. Technol. A 9 (1991) 3003.

[38] J. E. Rowe and H. Ibach, Phys. Rev. Lett. 31 (1973) 102.

[39] H. Ibach and J. E. Rowe, Surf. Sci. 43 (1974) 481.

[40] T. Sakurai and H. D. Hagstrum, Phys. Rev. B 14 (1976) 1593.

[41] C. J. Wu and E. A. Carter, Phys. Rev. B 46 (1992) 4651.

[42] Y. J. Chabal and K. Raghavachari, Phys. Rev. Lett. 53 (1984) 282.

[43] Y. J. Chabal and K. Raghavachari, Phys. Rev. Lett. 54 (1985) 1055.

[44] P. Gupta, V. L. Colvin and S. M. George, Phys. Rev. B 37 (1988) 8234.

[45] J. J. Boland, Advances in Physics 42 (1993) 129.

[46] K. Sinniah, M. G. Sherman, L. B. Lewis, W. H. Weinberg, J. T. J. Yates and K. C. Janda, Phys. Rev. Lett. 62 (1989) 567.

[47] K. Sinniah, M. G. Sherman, L. Lewis, W. H. Weinberg, J. T. J. Yates and K. C. Janda, J. Chem. Phys. 92 (1990) 5700.

[48] S. Ciraci, R. Butz, E. M. Oellig and H. Wagner, Phys. Rev. B 30 (1984) 711.

[49] J. J. Boland, Phys. Rev. Lett. 67 (1991) 1539.

[50] J. J. Boland, J. Vac. Sci. Technol. A 10 (1992) 2458.

[51] M. J. Bronikowski, Y. Wang, M. T. McEllistrem, D. Chen and R. J. Hamers, Surf. Sci. 298 (1993) 50.

[52] X. Chen, B. Cousins, M. McEllistrem and R. J. Hamers, Rev. Sci. Instrum. 63 (1992) 4308.

[53] R. S. Becker, G. S. Higashi, Y. J. Chabal and A. J. Becker, Phys. Rev. Lett. 65 (1990) 1917.

[54] R. M. Tromp, R. J. Hamers and J. E. Demuth, Phys. Rev. Lett. 55 (1985) 1303.

[55] R. J. Hamers, R. M. Tromp and J. E. Demuth, Phys. Rev. B 34 (1986) 5343.

[56] R. J. Hamers and U. K. Köhler, J. Vac. Sci. Technol. A 7 (1989) 2854.

[57] J. A. Appelbaum, G. A. Baraff and D. R. Hamann, Phys. Rev. B 14 (1976) 588.

[58] J. A. Appelbaum, G. Baraff, D. R. Hamann, H. D. Hagstrom and T. Sakurai, Surf. Sci. 70 (1978) 654.

[59] R. J. Hamers, R. M. Tromp and J. E. Demuth, Surf. Sci. 181 (1987) 246.

[60] R. J. Hamers, U. K. Kohler and J. E. Demuth, Ultramicroscopy 31 (1989) 10.

[61] O. L. Alerhand, A. N. Becker, J. D. Joannopoulos, D. Vanderbilt, R. J. Hamers and J. E. Demuth, Phys. Rev. Lett. 64 (1990) 2409.

[62] B. S. Swartzentruber, Y.-W. Mo, R. Kariotis, M. G. Lagally and M. B. Webb, Phys. Rev. Lett. 65 (1990) 1913.

[63] J. J. Boland, Personal Communication

[64] G. Brocks, P. J. Kelly and R. Car, Phys. Rev. Lett. 66 (1991) 1729.

[65] G. Brocks, P. J. Kelly and R. Car, Surf. Sci. 269/270 (1992) 860.

[66] J. D. Chadi, Phys. Rev. Lett. 59 (1987) 1691.

[67] R. J. Hamers, P. Avouris and F. Bozso, Phys. Rev. Lett. 59 (1987) 2071.

[68] P. Avouris, F. Bozso and R. J. Hamers, J. Vac. Sci. Technol. B 5 (1987) 1387.

[69] R. J. Hamers, P. Avouris and F. Bozso, J. Vac. Sci. Technol. A 6 (1988) 508.

[70] J. A. Appelbaum, G. A. Baraff and D. R. Hamann, Phys. Rev. B 15 (1977) 2408.

[71] J. A. Appelbaum, G. A. Baraff and D. R. Hamann, Phys. Rev. B 15 (1977) 2006.

[72] J. A. Appelbaum, G. A. Baraff and D. R. Hamann, Phys. Rev. Lett. 35 (1975) 729.

[73] C. J. Wu and E. A. Carter, Chem. Phys. Lett. 185 (1991) 172.

[74] A. Vittadini, A. Selloni and M. Casarin, Surf. Sci. 289 (1993) L625.

[75] R. J. Hamers, U. K. Kohler and J. E. Demuth, J. Vac. Sci. Technol. A 8 (1990) 195.

[76] Y.-W. Mo, B. S. Swartzentruber, R. Kariotis, M. B. Webb and M. G. Lagally, Phys. Rev. Lett. 63 (1989) 2393.

[77] J. J. Boland, Phys. Rev. Lett. 65 (1990) 3325.

[78] D. J. Chadi, Phys. Rev. Lett. 43 (1979) 43.

[79] M. J. Bronikowski, Y. Wang and R. J. Hamers, Phys. Rev. B 48 (1993) 12361.

[80] C. M. Greenlief, S. M. Gates and P. A. Holbert, J. Chem. Phys. 92 (1990) 3144.

[81] C. M. Greenlief, S. M. Gates and P. A. Holbert, Chem. Phys. Lett. 159 (1989) 202.

[82] H. Kobayashi, K. Edamoto, M. Onchi and M. Nishijima, J. Chem. Phys. 78 (1983) 7429.

[83] C. Isobe, H. C. Cho and J. E. Crowell, Surf. Sci. 295 (1993) 99.

[84] R. Imbihl, J. E. Demuth, S. M. Gates and B. A. Scott, Phys. Rev. B 39 (1989) 5222.

[85] C. J. Wu and E. A. Carter, Phys. Rev. B 45 (1992) 9065.

[86] J. Y. Tsao, E. Chason, U. Koehler and R. J. Hamers, Phys. Rev. B 40 (1989) 11951.

FIGURE CAPTIONS

Fig. 1: STM Images showing room temperature adsorption of Si_2H_6 on Si(001)-(2X1) surface. (a) clean surface before exposure, including a monatomic step; (b) same region as in (a), after 0.1 Langmuir Si_2H_6 exposure. Several adsorption-induced protrusions are indicated by arrows, and a region of dimer buckling induced by H adsorption is outlined by the box. Image dimensions 240 Å X 240 Å, V_s = -2.2 V, I_t = 0.5 nA.

Fig. 2: Change in surface appearance with applied voltage for a 20 Å X 40 Å region of a disilane-exposed Si(001) surface which includes both adsorbed SiH_2 groups and H atoms.
(a) positive sample bias, imaging the unoccupied surface states (V_s = +2.0 V, I_t = 0.3 nA)
(b) negative sample bias, imaging the occupied surface states (V_s = -2.5 V, I_t = 0.3 nA)
(c) Surface model, indicating the geometries and chemical identity of the observed features.

Fig. 3: Sequential images of Si(001) obtained while simultaneously dosing with disilane at room temperature. (a) corresponds to surface dosed with 0.1 Langmuir before tunneling; other images are taken 230 seconds apart during continuous exposure. In (3c), several SiH_3 groups are indicated by arrows. Dimensions 200 Å X 200 Å, V_s = -2.2 V, I_t = 0.5 nA.

Fig. 4: Sequential images of Si(001) surface showing adsorption of SiH_2 and SiH_3, and the dissociation reaction $SiH_3(ads) \rightarrow SiH_2(ads) + H(ads)$
(a) shows the clean Si(001) surface before exposure to Si_2H_6
(b) same area as (a) after exposure to 0.1L Si_2H_6 exposure at 300 K, showing adsorbed SiH_2 group (upper) and SiH_3 group (lower).
(c) same region as (a) and (b), acquired 8 minutes after (b), showing shift in bonding location as SiH_3 group dissociates to SiH_2, and the appearance of atomic-sized depression due to H atom adsorption. Dimensions: 47 Å X 47 Å, with V_s = -2.2 V, I_t = 0.5 nA.

Fig. 5: Image of Si(001) surface after exposure to 0.2L Si_2H_6 at 300 K and then annealed at 470K for 2 min.
(a) Overall structure after the treatment, showing SiH_2 groups and several types of dimer structures. Dimensions 175 Å X 175 Å, with V_s = -2.0 V, I_t = 0.5 nA;
(b) Higher-resolution image of region from (5a), showing different bonding locations of three types of dimer structures.. Dimensions: 70 Å X 70 Å, with V_s = -2.0 V, I_t = 0.5 nA.

Fig. 6: Model for four possible Si=Si ad-dimer structures which achieve four-fold coordination for adsorbing silicon atoms.. The structure shown in (b), (c) and (d) are found in fig. 5.

Fig. 7: STM image of Si(001) surface showing several types of dimer structures. The surfaces were exposed to 0.2L Si_2H_6 at 300 Kelvin, then annealed at 470K for only 10 sec; .V_s = -2.0 V, I_t = 0.5 nA for both images.
(a) Dimensions 30 Å X 67 Å
(b) Dimensions 48 Å X 85 Å
(c) Structural model for the features observed in (a) and (b).

Fig. 8 : (a) Image of Si(001) surface prepared by exposure to 0.2L Si_2H_6 at 300 K, then annealed at 470K for 2min. Several features are labeled and described in the text. Dimensions 142 Å X 142 Å, V_s = -2.0 V, I_t = 0.5 nA;
(b) Height profiles measured across paired SiH_2 groups and across individual SiH_2 groups along the line shown on (a), showing they have the same height.

Fig. 9: Simple molecular-orbital energy level diagrams for different structures on Si(001),
(a) electronic structure for bulk-terminated, unreconstructed Si(001);
(b) electronic structure after 2X1 dimer reconstruction;
(c) electronic structure after adsorption of one H atom per dimer
(d) electronic structure after adsorption of two H atoms per dimer to form the monohydride phase

Fig. 10: Identification of the H-Si-Si-H monohydride phase.

(a) STM image of Si(001) surface after exposure to 0.6 L Si_2H_6 at 300 K, then annealed at 660K for 5min, including a monatomic step. Regions of the monohydride phase are observed on both upper and lower terraces, and in some cases on the epitaxial islands. Dimensions: 190 Å X 190 Å, V_S = -1.9 V, I_t = 0.5 nA.
(b) Chemical map corresponding to (a); paired circles are monohydride dimers, and ellipses are "clean" Si=Si dimers. The topmost layers use open symbols, the lowest layers use filled symbols.

Fig. 11(a): Si(001) surface after exposure to 0.6 L Si_2H_6 at 300 K, then annealed at 660K for 5 min. showing both clean dimers and monohydride dimers; Dimensions 190 Å X 190 Å, V_S = -3.0 V, I_t = 0.5 nA;
(b): Enlarged view of area outlined by rectangular box in fig. 11a, showing that monohydride dimers appear lower and show a slight minimum at the dimer center. Dimensions 31Å X 52Å, V_S = -3.0 V, I_t = 0.5 nA;
(c): Height profile measured along the line between the two arrows in (a), showing that at this bias monohydride dimers appear about 1 Å lower than Si=Si dimers, and that monohydride dimers show two protrusions across the dimer direction with a minimum at the center, while "clean" dimers show only a single maximum.

Fig. 12: Apparent height difference between "clean" Si=Si dimers and monohydride dimers, obtained from repeated measurements over the area shown in fig. 11 at different bias voltages.

Fig. 13: Images of Si(001) after exposure to 0.2L Si_2H_6 at 300K and annealed at 430K for 5 min.
(a) shows SiH_2 groups, adsorbed H atoms, and individual Si=Si dimers; Dimensions 190 Å X 220 Å, V_S = -2.0 V, I_t = 0.5 nA;
(b) shows a similar region including a step, demonstrating that there is not preferential diffusion or reaction at step edges. Dimensions 190 Å X 237 Å, V_S = -2.0 V, I_t = 0.5 nA.

Fig. 14: Si(001) surface after exposure to 0.2 L Si_2H_6 at room temperature, then annealed at 470K for 2 min. SiH_2 groups and several kinds of dimer structures are clearly visible; small regions of monohydride phase appear like vacancies

under these image processing conditions. Dimensions 354 Å X 477 Å, V_S = -2.0 V, I_t = 0.5 nA.

Fig. 15: Si(001) surface after exposure to 0.2 L Si_2H_6 at room temperature, then annealed at 470K for 2 min. The arrow points to one small region of approximately 8 dimers of the monohydride phase, which appear lower than "clean" dimers. Several other small monohydride regions can be observed near the top and at lower left. Dimensions 108 Å X 108 Å, V_S = -2.0 V, I_t = 0.5 nA.

Fig. 16: Si(001) after exposure to 0.2L Si_2H_6 at room temperature, then annealed at 505K for 5min. Dimensions 200 Å X 220 Å, V_s = -1.6 V, I_t = 0.5 nA;

Fig. 17: STM image of a single region of the Si(001) surface which was exposed to 0.2 L Si_2H_6 and then annealed to 505 K for 5 min, showing how the surface appears more ordered when imaged at high bias voltages.
(a): V_S = -1.5 V, I_t = 0.5 nA, 162Å X 162Å;
(b): V_S = -2.5 V, I_t = 0.5 nA, 162Å X 162Å .

Fig. 18: Si(001) surface after exposure to 0.2 L Si_2H_6 at 300 K, then annealed at 540K for 5min. Anisotropic Si "dimer string" islands have been formed on the surface, coexisting with regions of monohydride and a few SiH_2 groups.
(a): Large scale image, Dimensions 810 Å X 1050 Å, V_S = -1.8 V, I_t = 0.65 nA
(b): Atomically-resolved close-up, Dimensions 185Å X 206Å, V_S = -1.8 V, I_t = 0.5 n A

Fig. 19: Si(001) surface after exposure to 0.2 L Si_2H_6 at room temperature, then annealed at 660K for 5min. Compared with fig. 18, the islands are longer and farther apart. Small regions of the monohydride phase appears as small depressions under these imaging conditions. Dimensions 708 Å X 820 Å, V_S = -1.8 V, I_t = 0.65 nA.

Fig. 20: Si(001) surface after exposure to 0.2 L Si_2H_6 at room temperature, then annealed at 660K for 5min.
(a) Overall image including monatomic steps. No preferential diffusion or reaction at the step edge is evident at this temperature. The arrow points to an epitaxial dimer of the monohydride phase; this dimer appears 1.2 Å lower than

its adjacent epitaxial "clean" dimers, and shows a minimum at the center of the dimer bond. Dimensions 200 Å X 214 Å, V_S = -1.6 V, I_t = 0.8 nA;
(b) Enlarged view of region including monohydride epitaxial dimer; Dimensions: 58 Å X 58 Å.

Fig 21: STM image o. Si(001) surface after exposure to 0.6L Si_2H_6 at room temperature, then annealed at 630K for 5min. At this coverage, the monohydride phase can be seen on both the substrate and on the epitaxial islands. (a) shows that the dimer strings have an aspect ratio of approximately 3:1. Dimensions 770 Å X 554 Å, V_S = -2.6 V, I_t = 0.3 nA.
(b) shows a high-resolution image under similar conditions, showing that the monohydride phase can be observed both on the substrate and on the epitaxial islands. Dimensions 177 Å X 177 Å, V_S = -2.6 V, I_t = 0.3 nA

Fig. 22: STM image of Si(001) surface, including a monatomic step, after exposure to 0.6 L Si_2H_6 at 300 K and then annealed at 660K for 5min.
(a) large-view image showing that monohydride phase is clearly visible on both substrate and on epitaxial islands. Dimensions 270Å X 340Å. V_S = -1.9 V, I_t = 0.5 nA
(b) Enlarged view of rectangular region from (a), showing that monohydride dimers occur near the center of epitaxial dimer strings, appear 1.2 Å lower than "clean" dimers, and show a minimum at the center of the dimer bond. Dimensions 69 Å X 131 Å.

Fig. 23: Large Si islands formed by exposure of Si(001) surface to 0.6L Si_2H_6 at 300 K, then annealing at 700K for 5 min.. "AP1" and "AP2" denote the two types of antiphase boundaries formed when islands intersect each other or terrace edges. At this temperature, all the hydrogen has desorbed. The silicon islands are anisotropic with an aspect ratio between 2:1 and 3:1, consistent with studies performed by solid phase epitaxy. Dimensions 770 Å X 860 Å, V_S = -2.6 V, I_t = 0.4 n A

Fig. 24: Models depicting proposed mechanisms for the decomposition of SiH_2(ads) and initial formation of Si=Si ad-dimers
(a) mechanism proposed in[16, 36];
(b) mechanism proposed from this study.

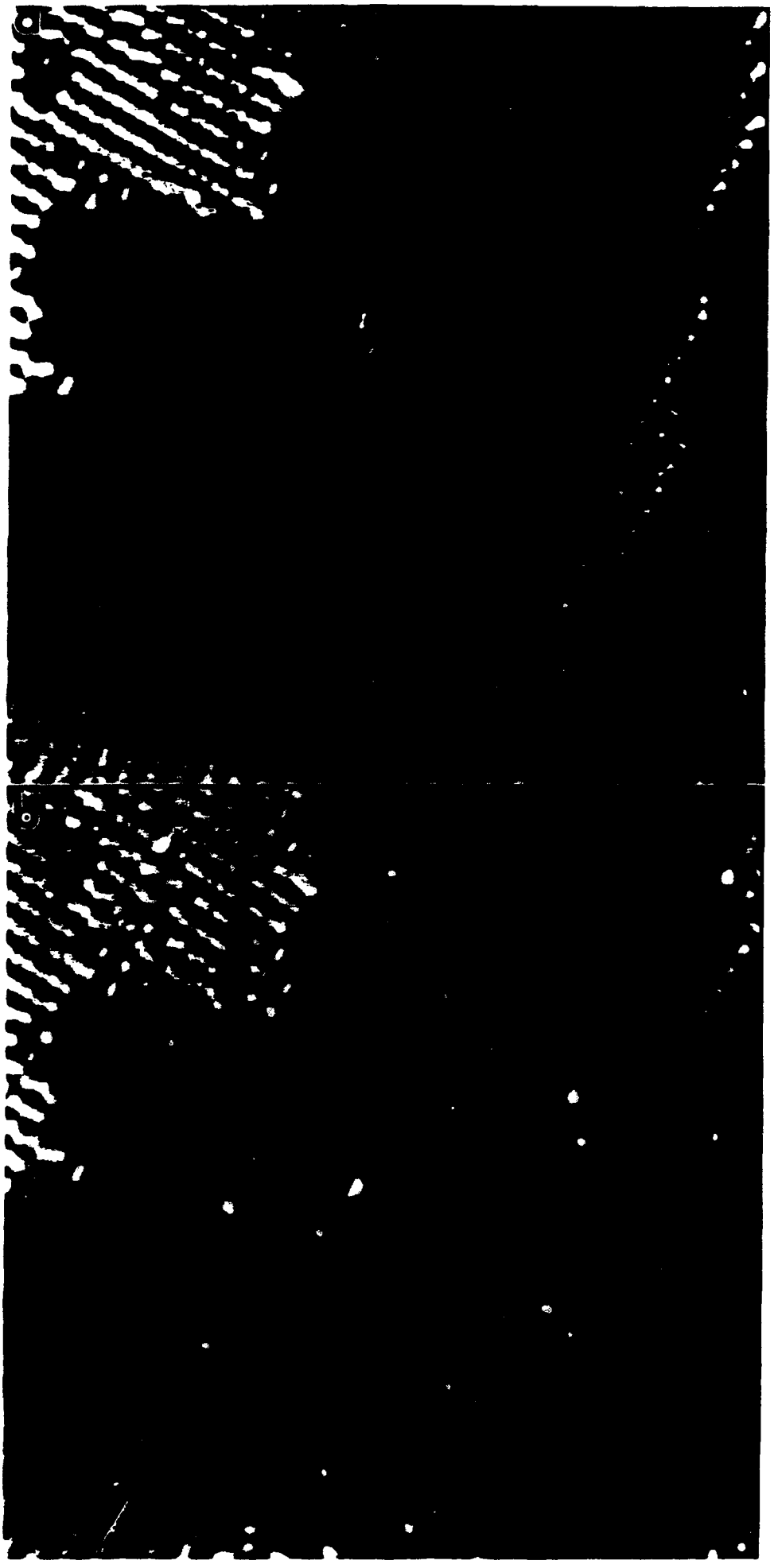

Wing

Fig

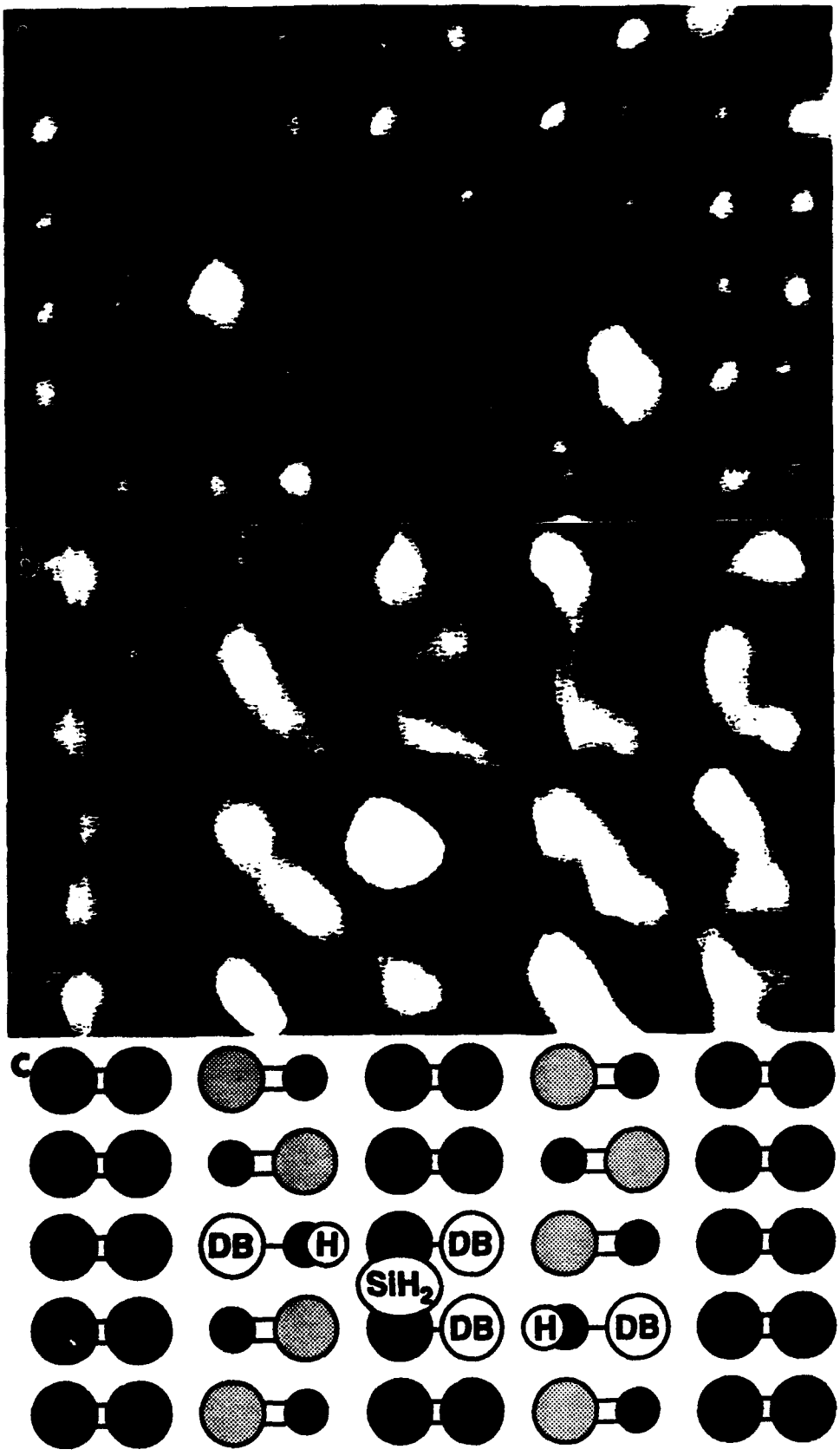
DB
H
DB
SiH2
DB
H
DB

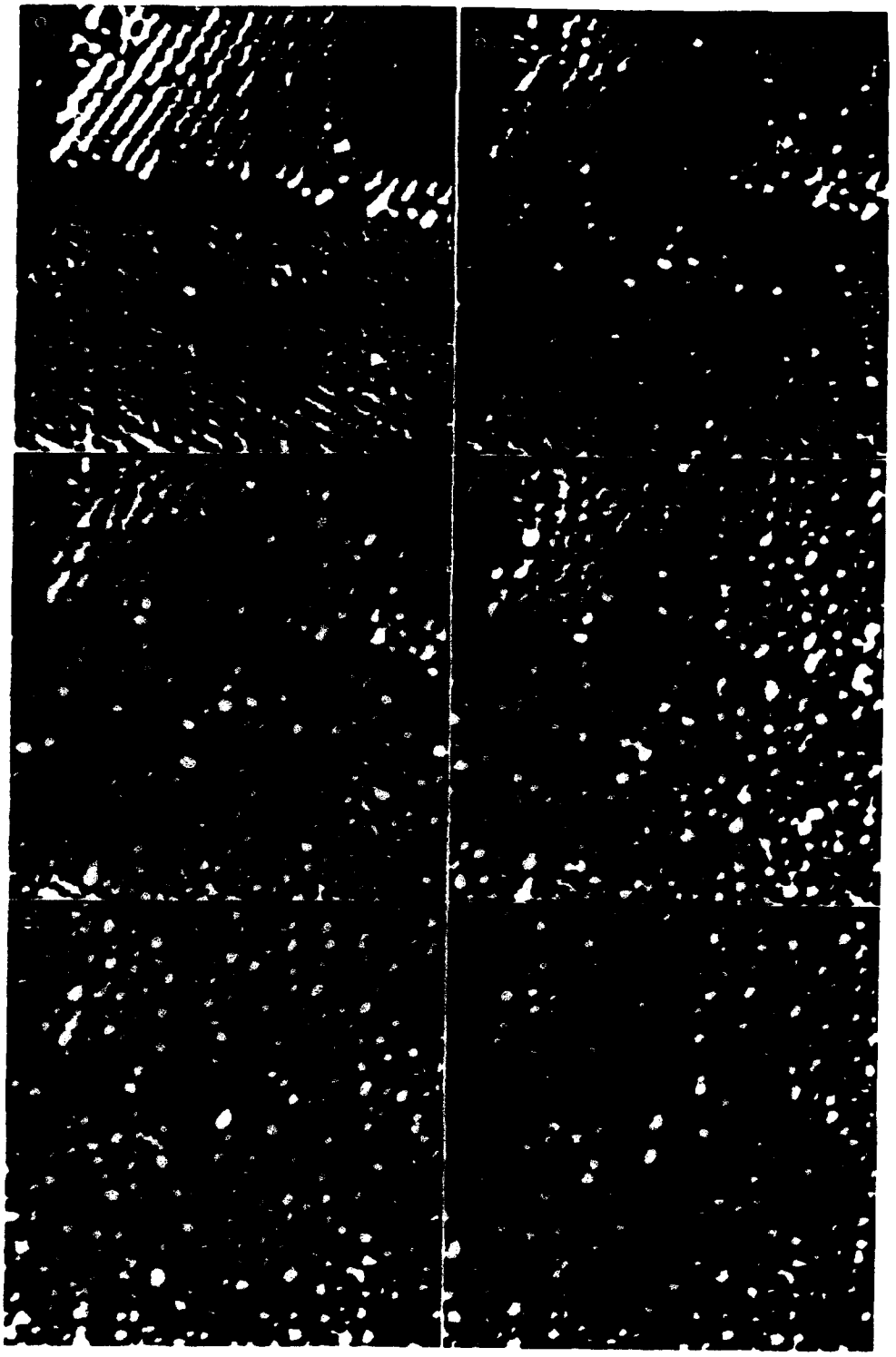

Wang et
Fig 3

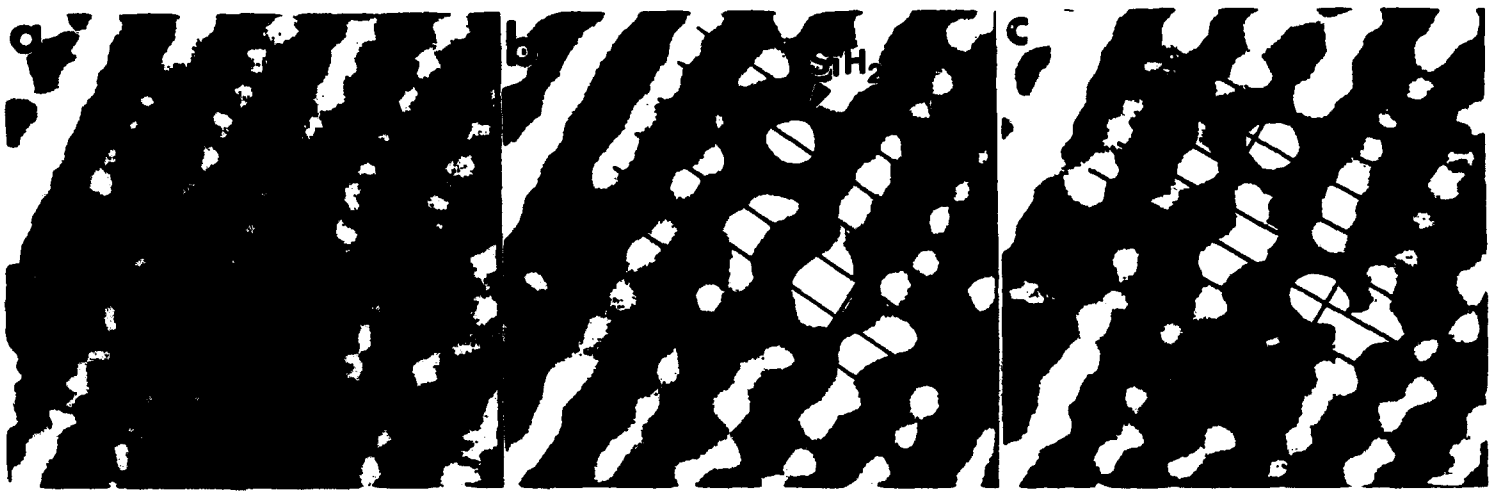

Wang et
Fig 4

Wang
F5

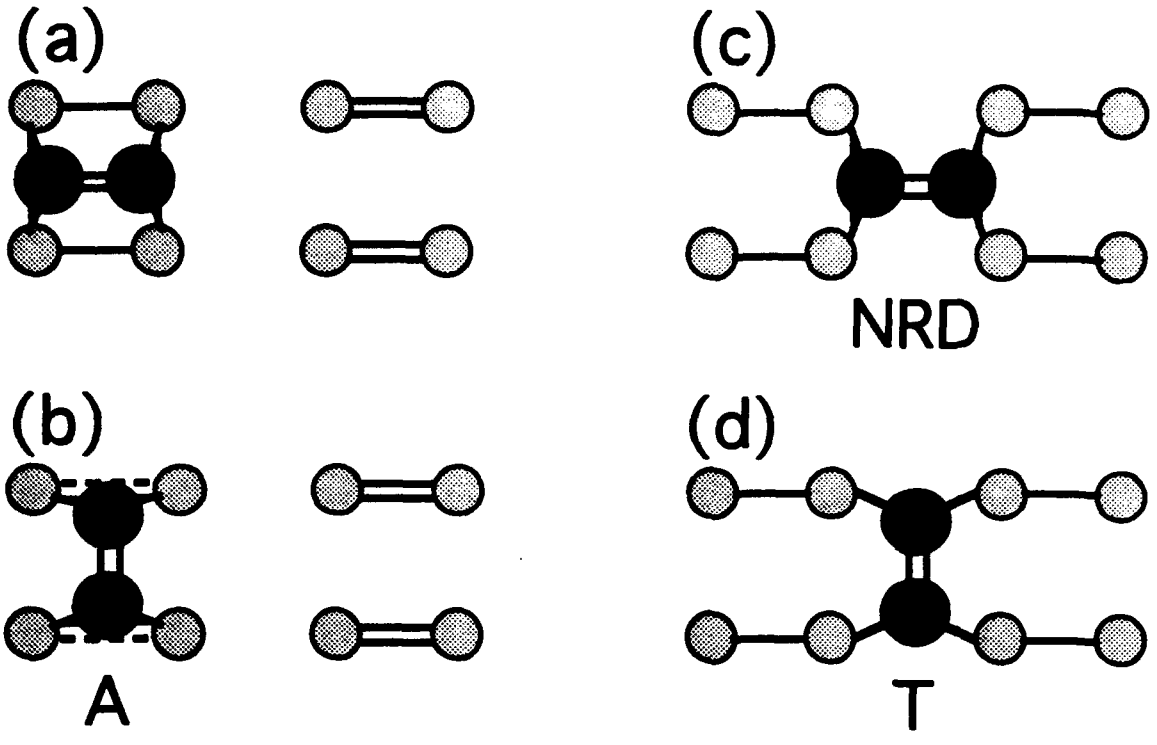

(Wang et al
Fig 6

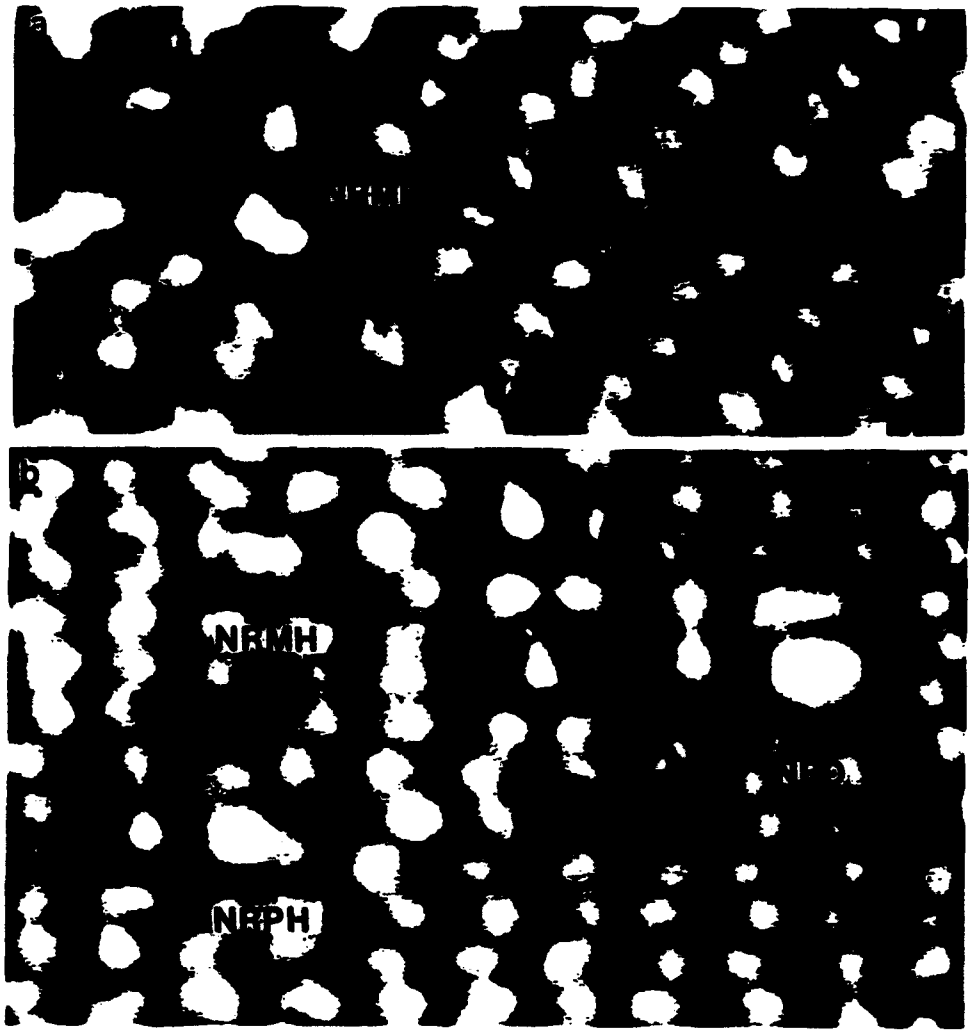
b
NBMH
NBPH

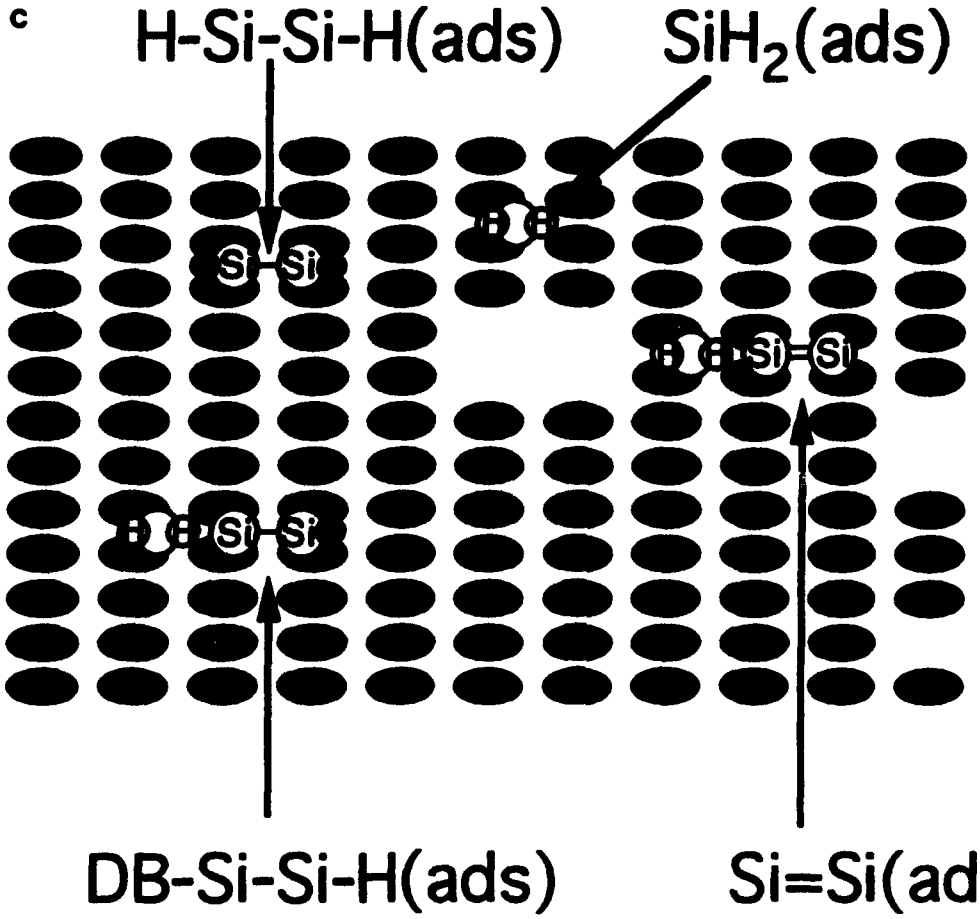
c
H-Si-Si-H(ads)
SiH2(ads)
Si-Si
B
Si=Si
DB-Si-Si-H(ads)
Si=Si(ads)

Fig. 7

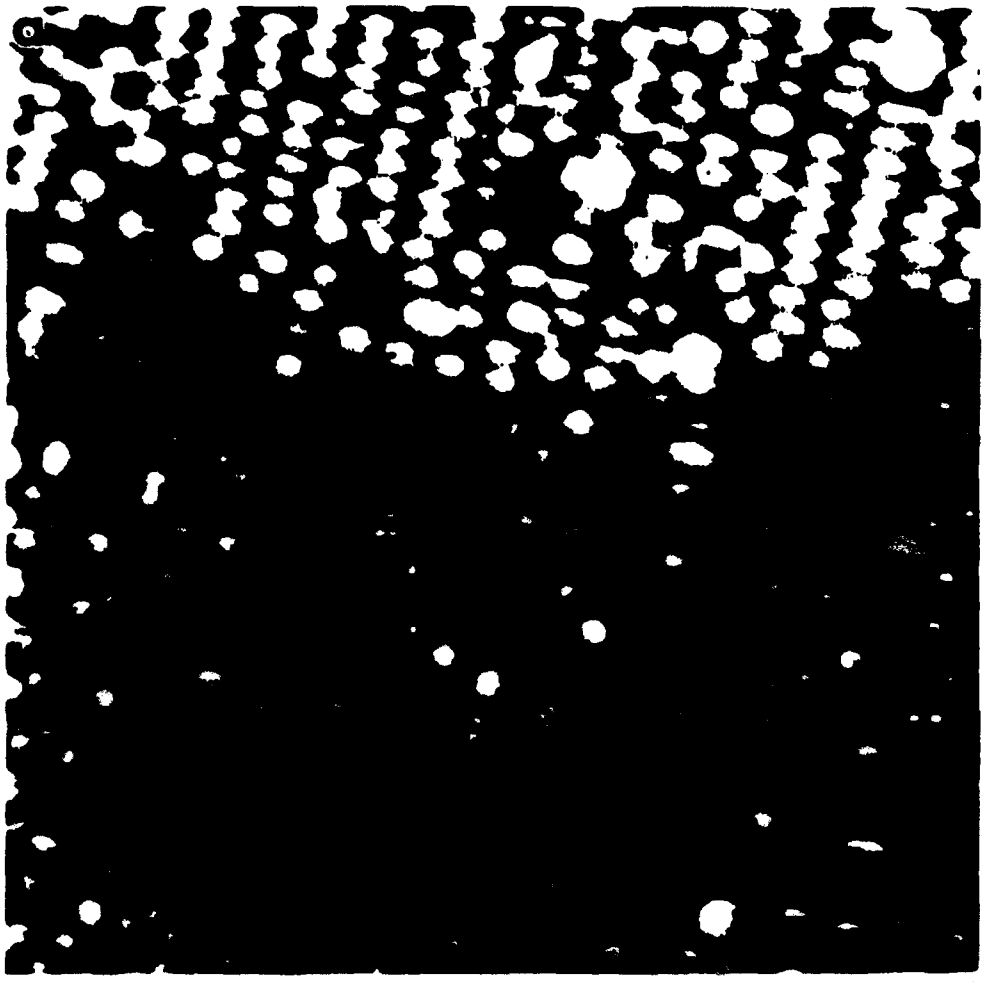

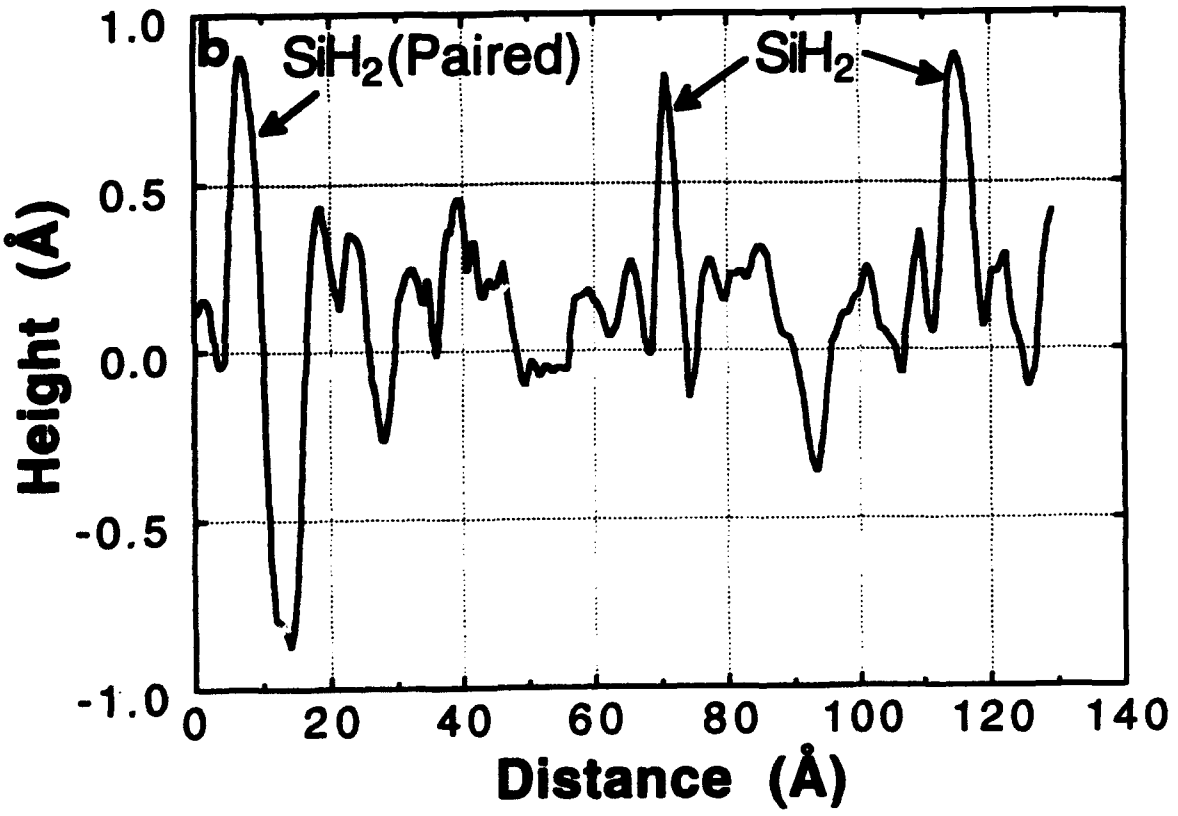
b
SiH2(Paired)
SiH2
1.0
0.5
0.0
-0.5
-1.0
Height (Å)
0
20
40
60
80
100
120
140
Distance (Å)

Fig. 9

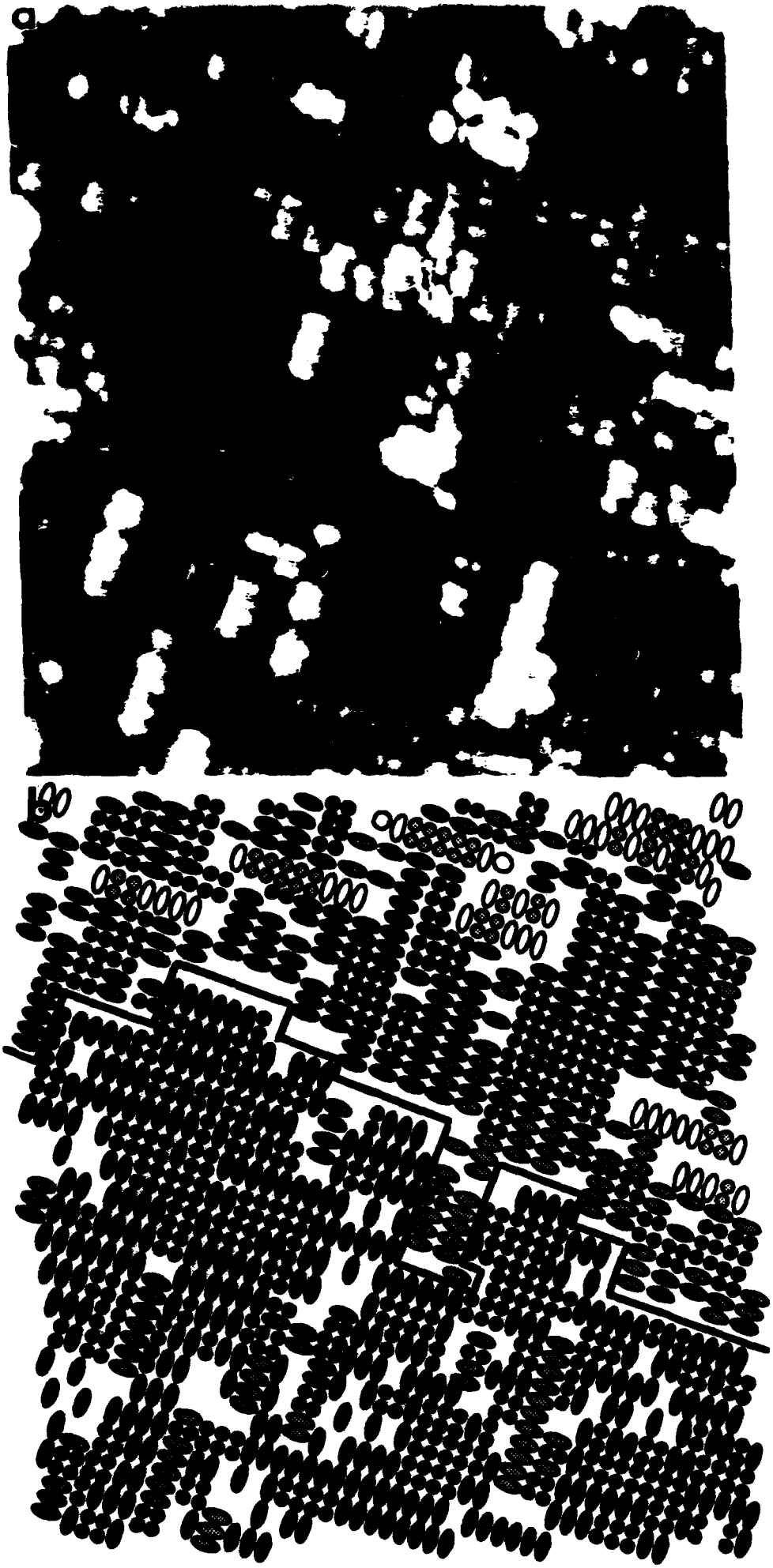

Wang
Fig

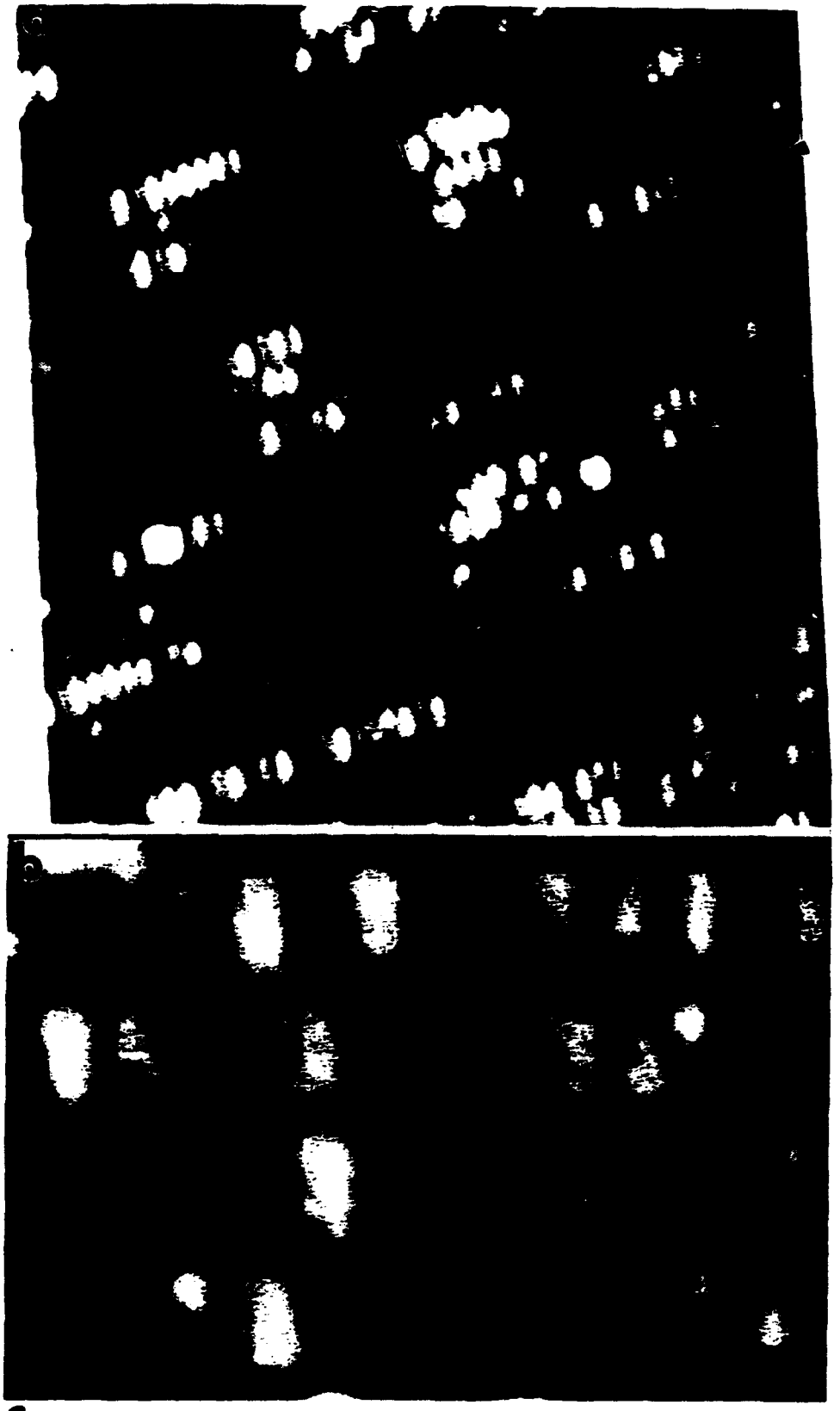

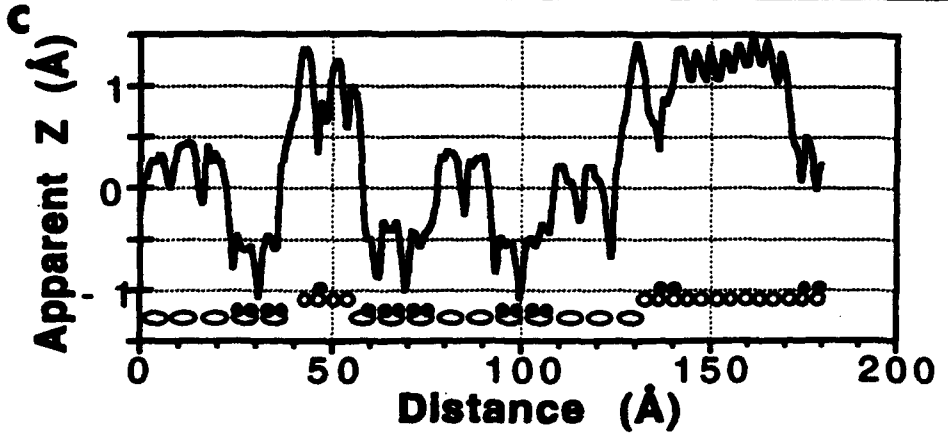

Wang et a
Fig. 1

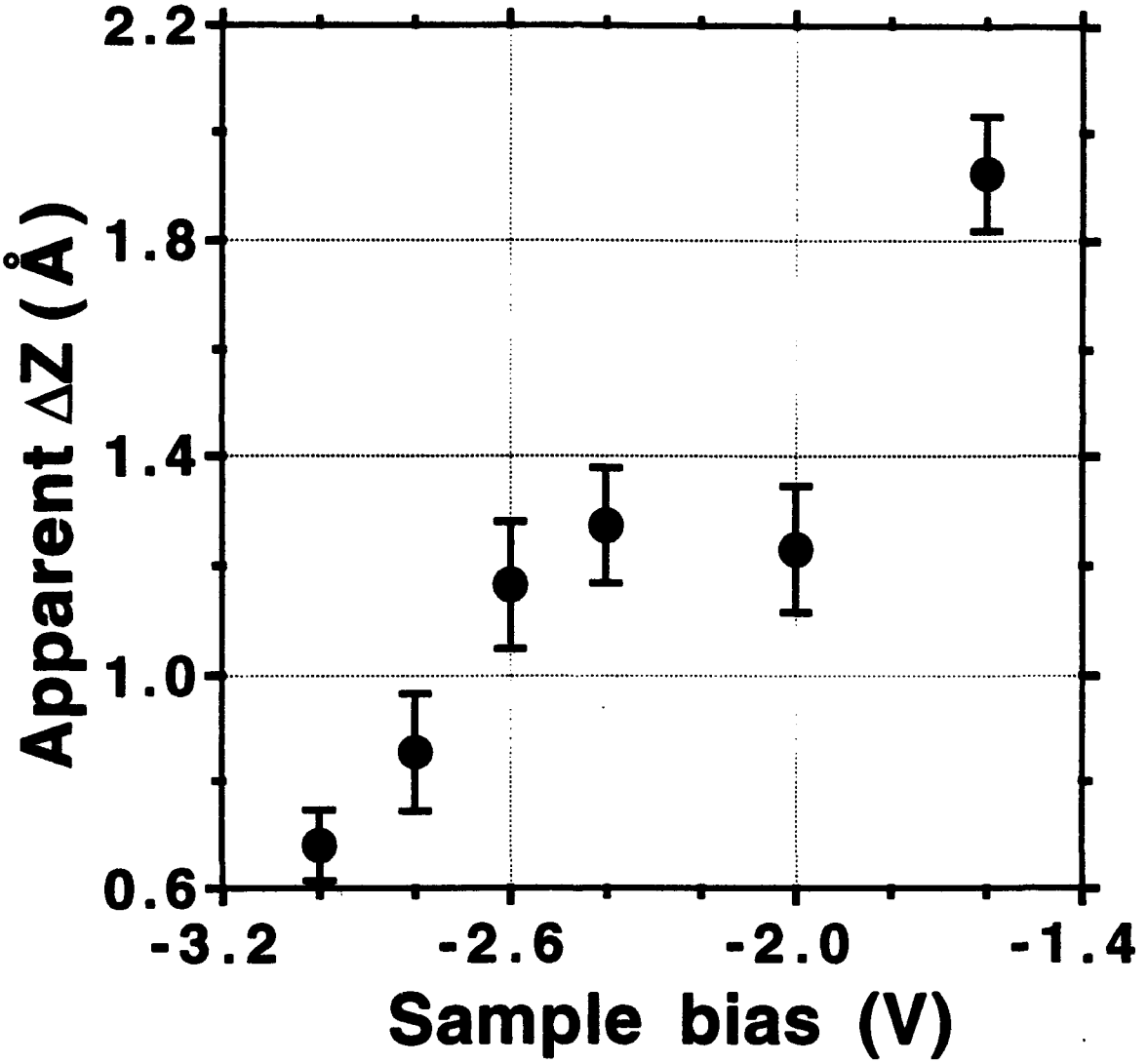

Wang et
Fig 12

Wing of
Fig 1

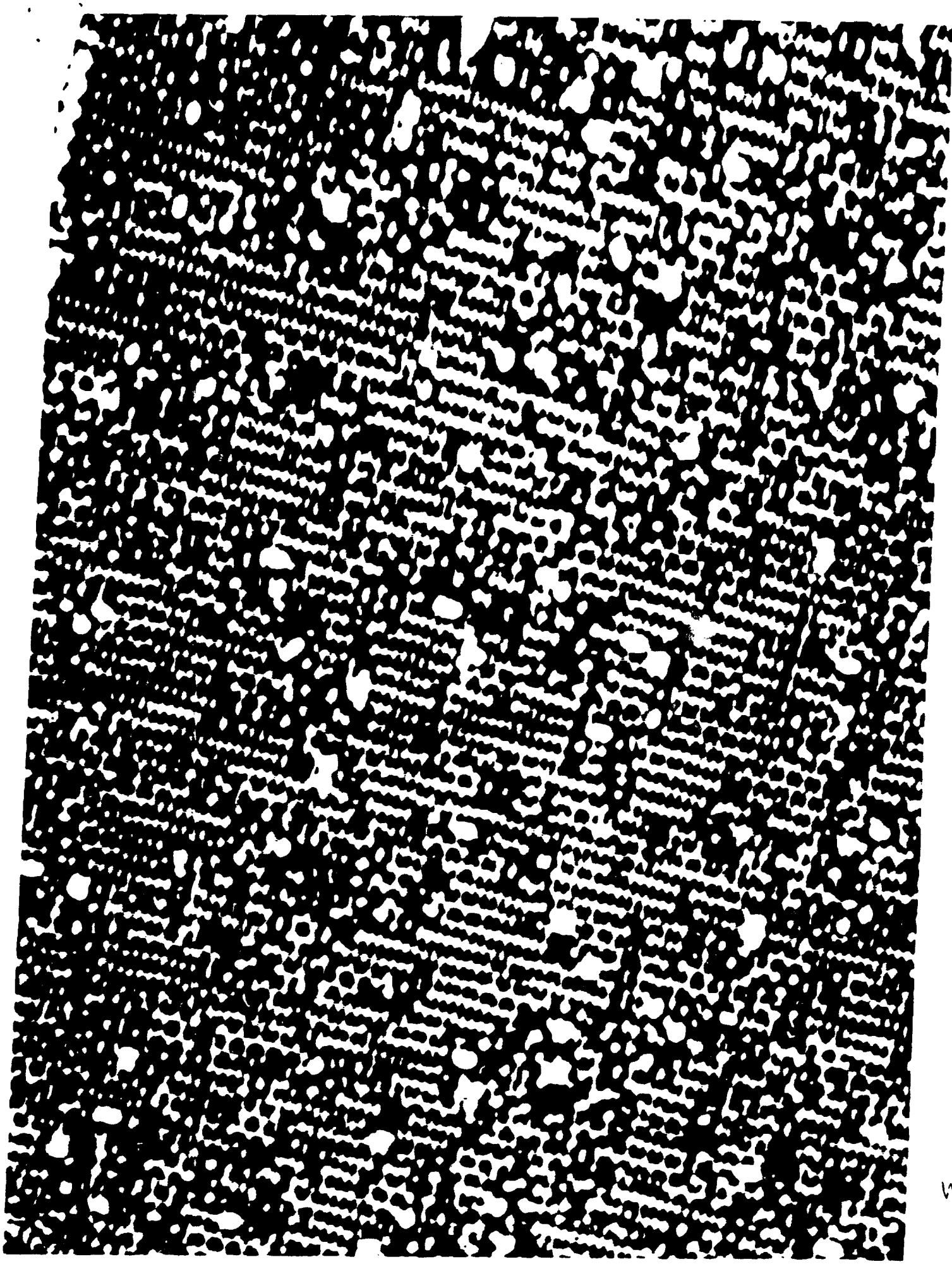

Wing.
F.5.

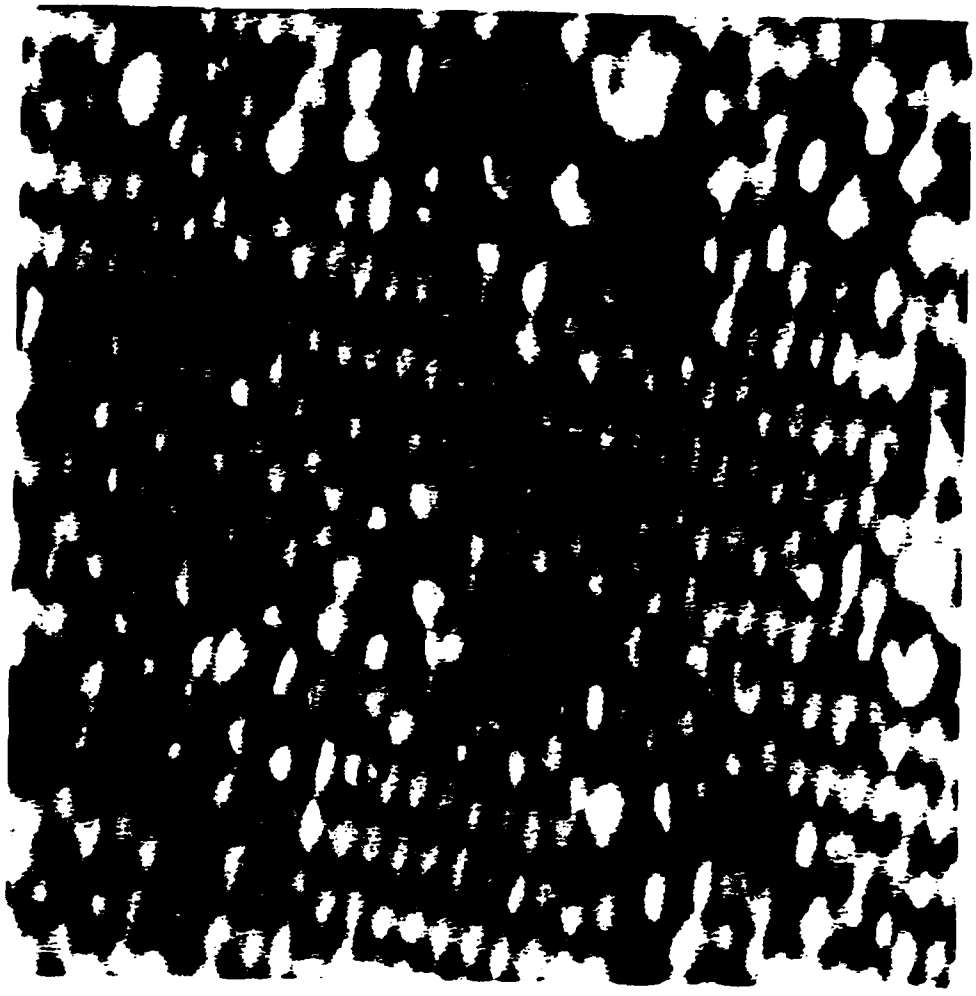

Wang et
Fig. 15

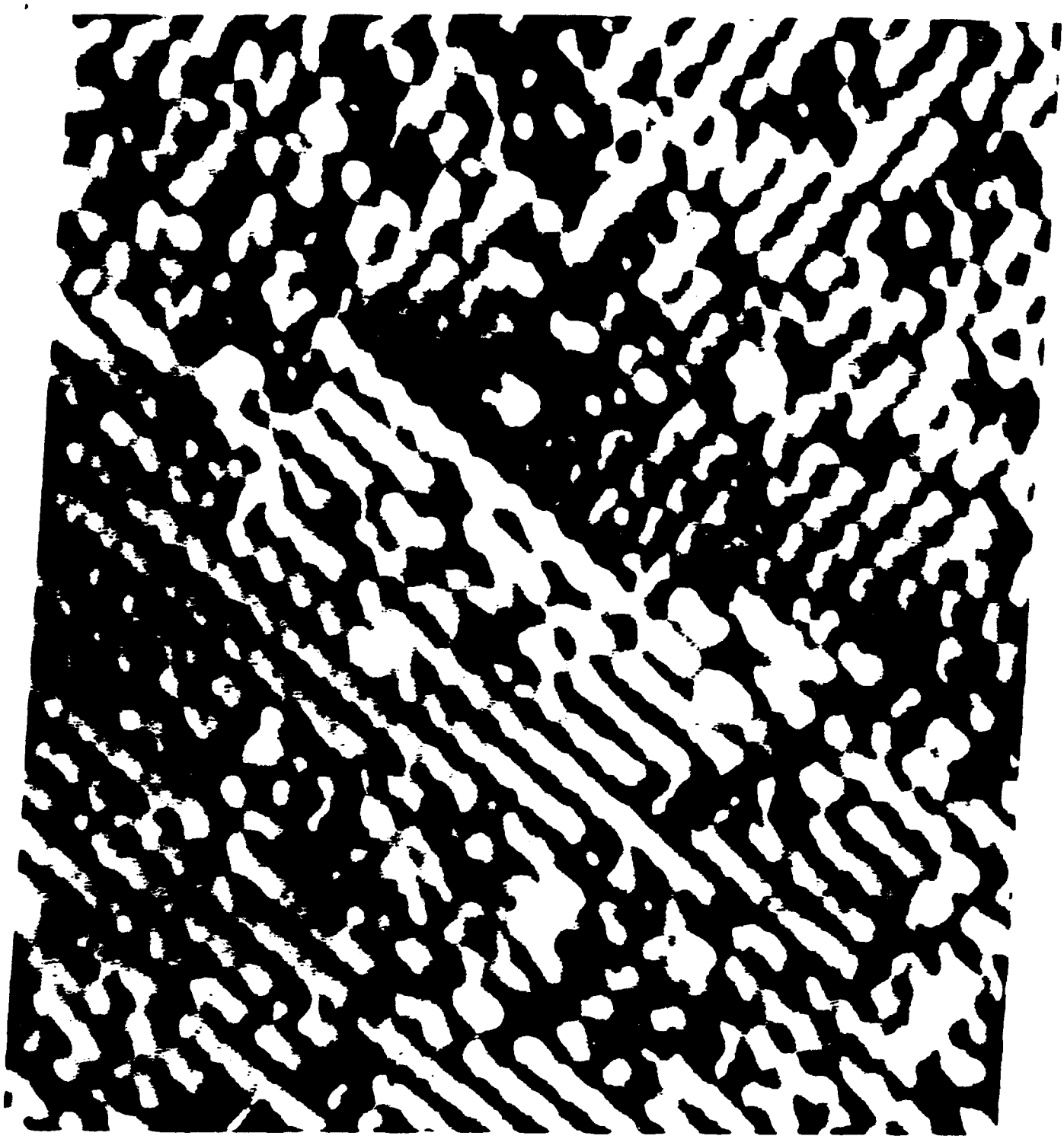

Wang et
F 3

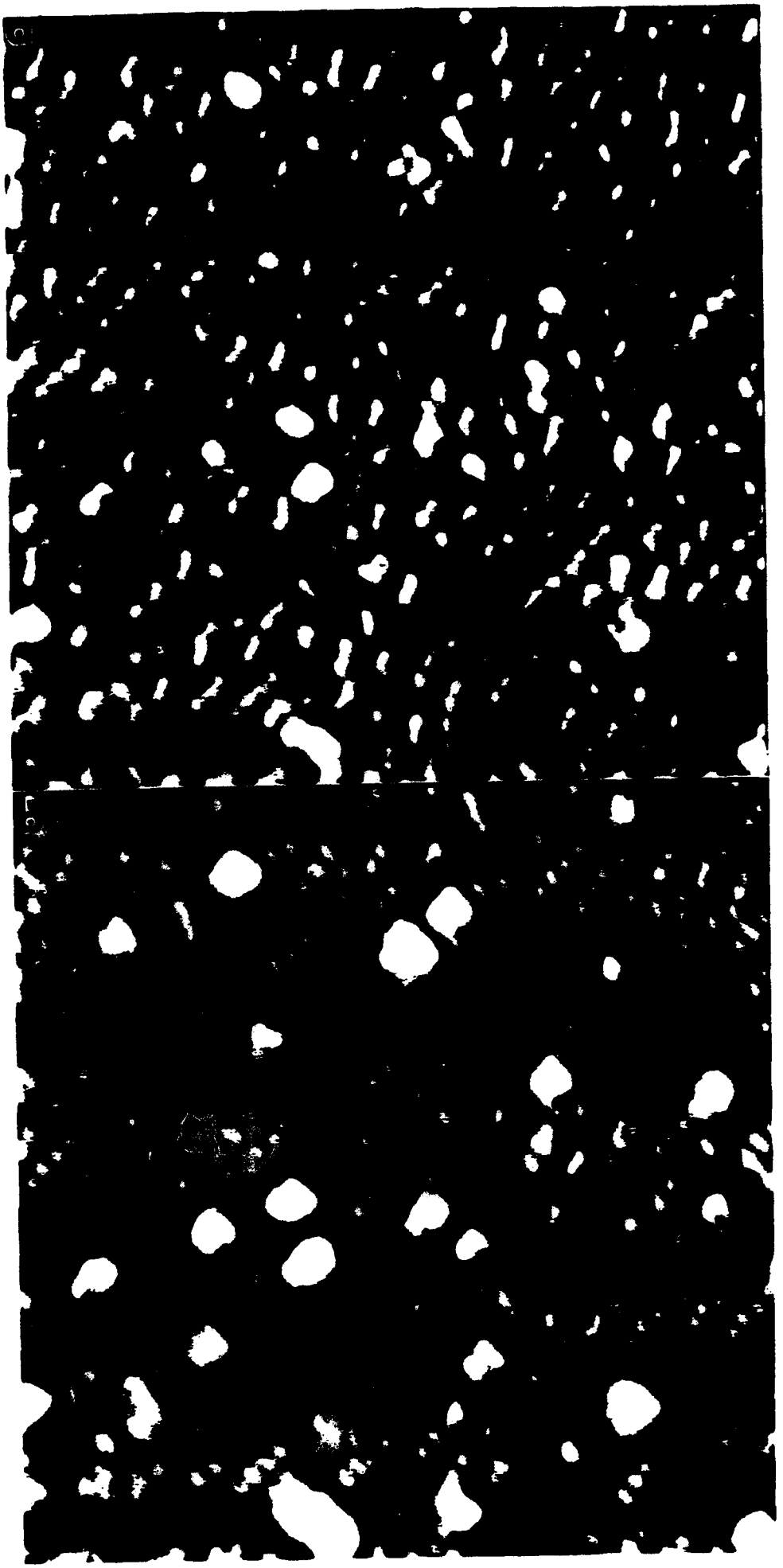

Wang
Fig

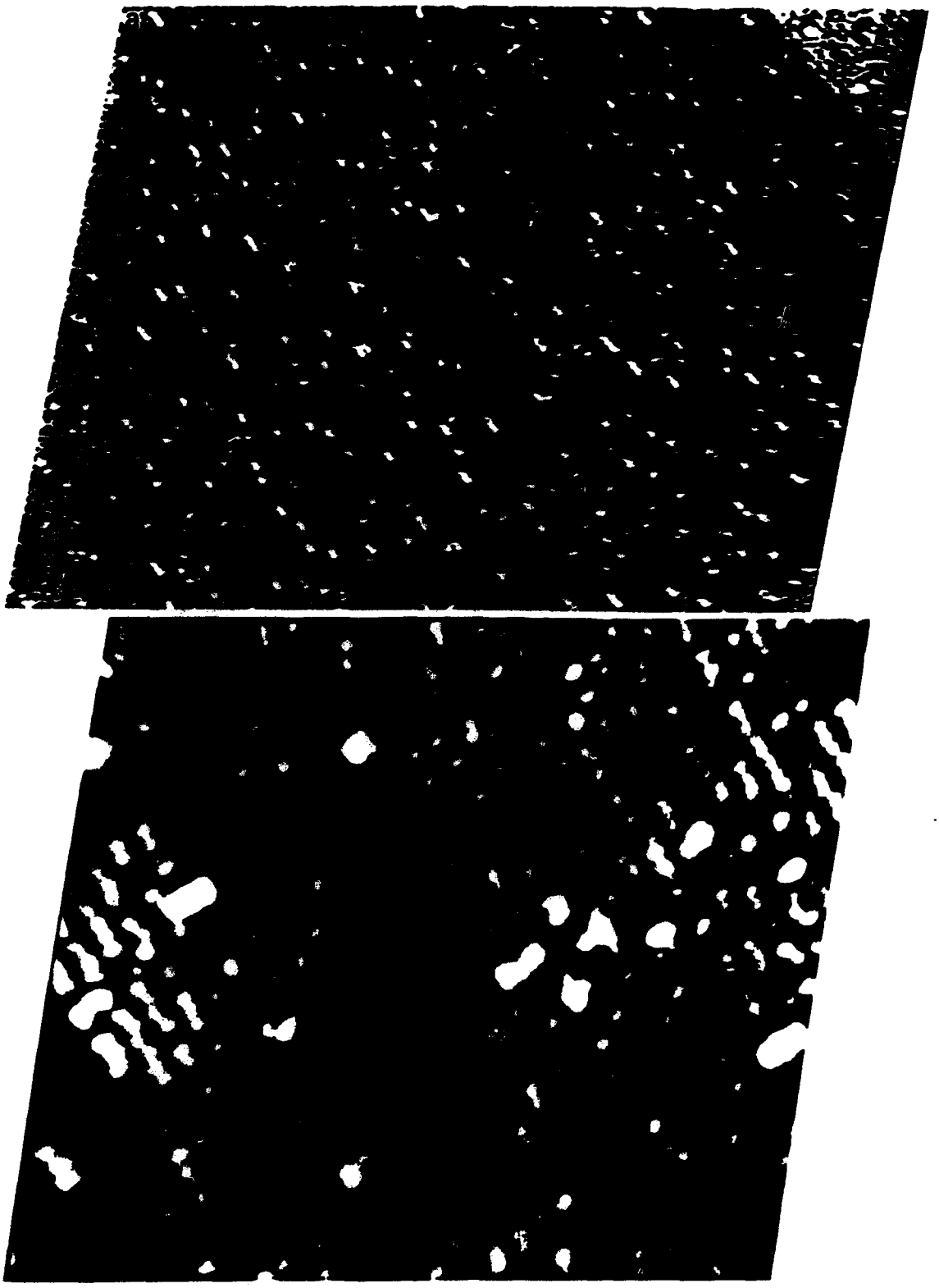

Wang et.
Fig 1

Wang e
Fig.

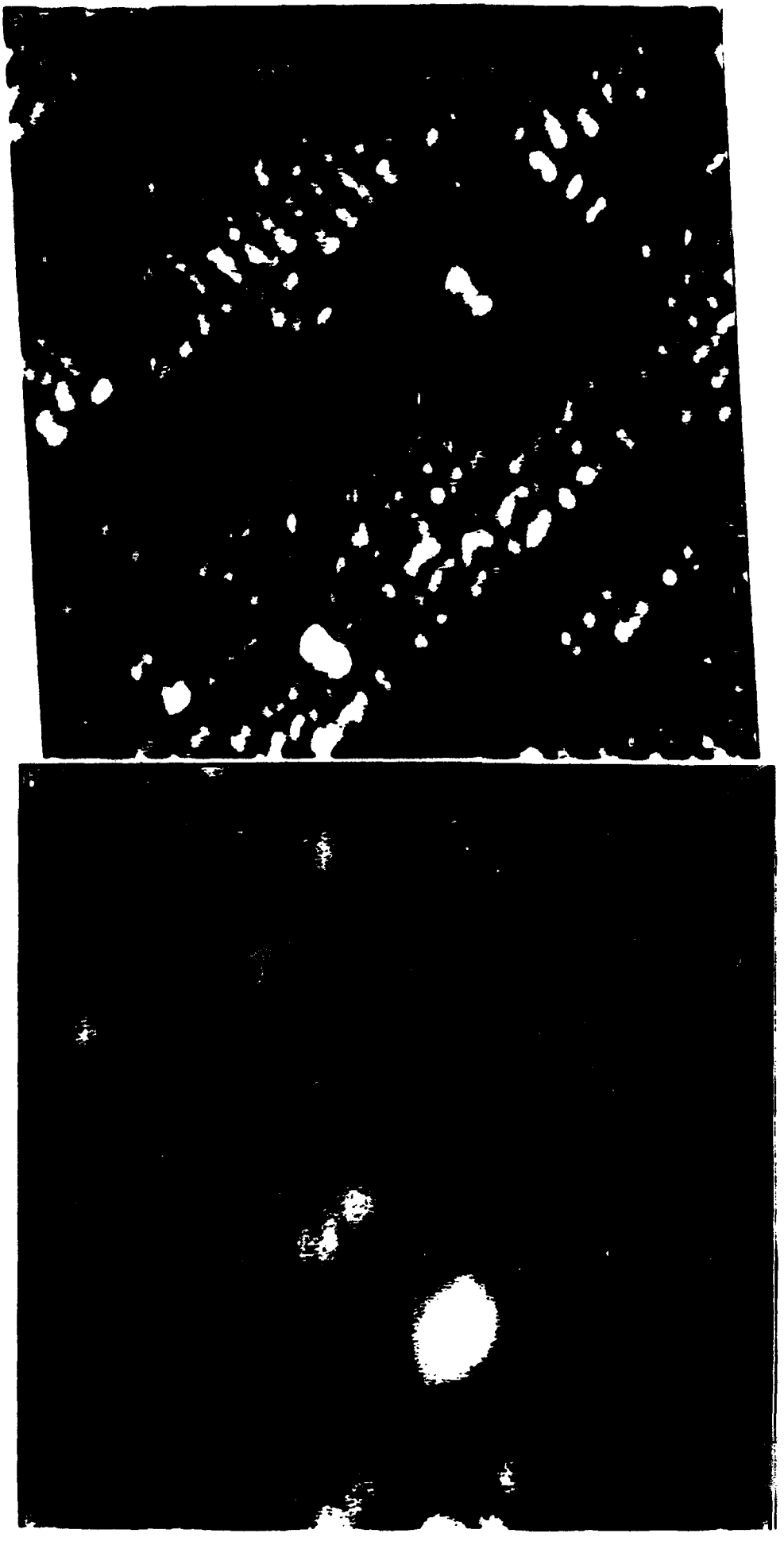

Wang et.
Fig. 2c

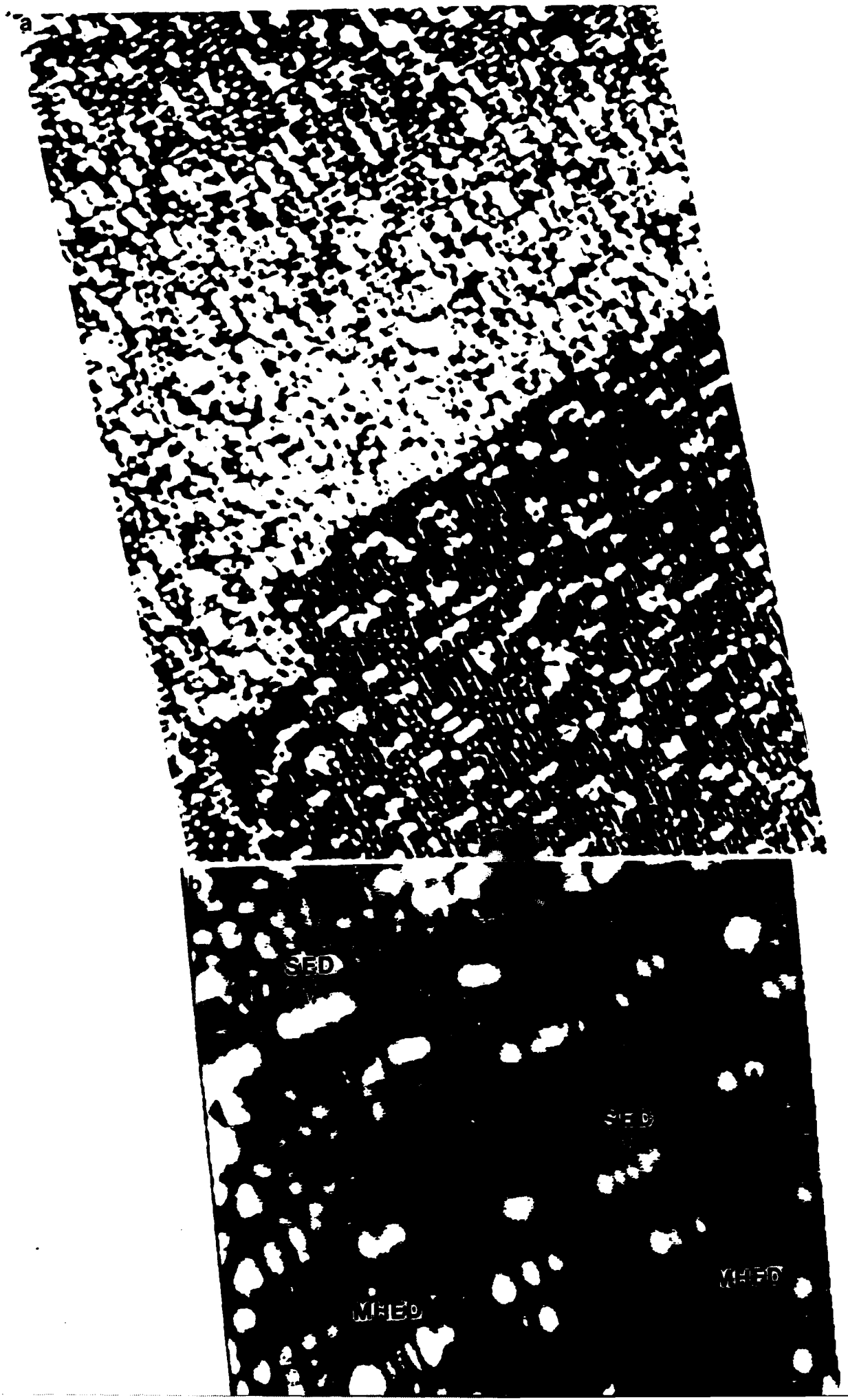

Wang
Fi

Wang et
Fig =

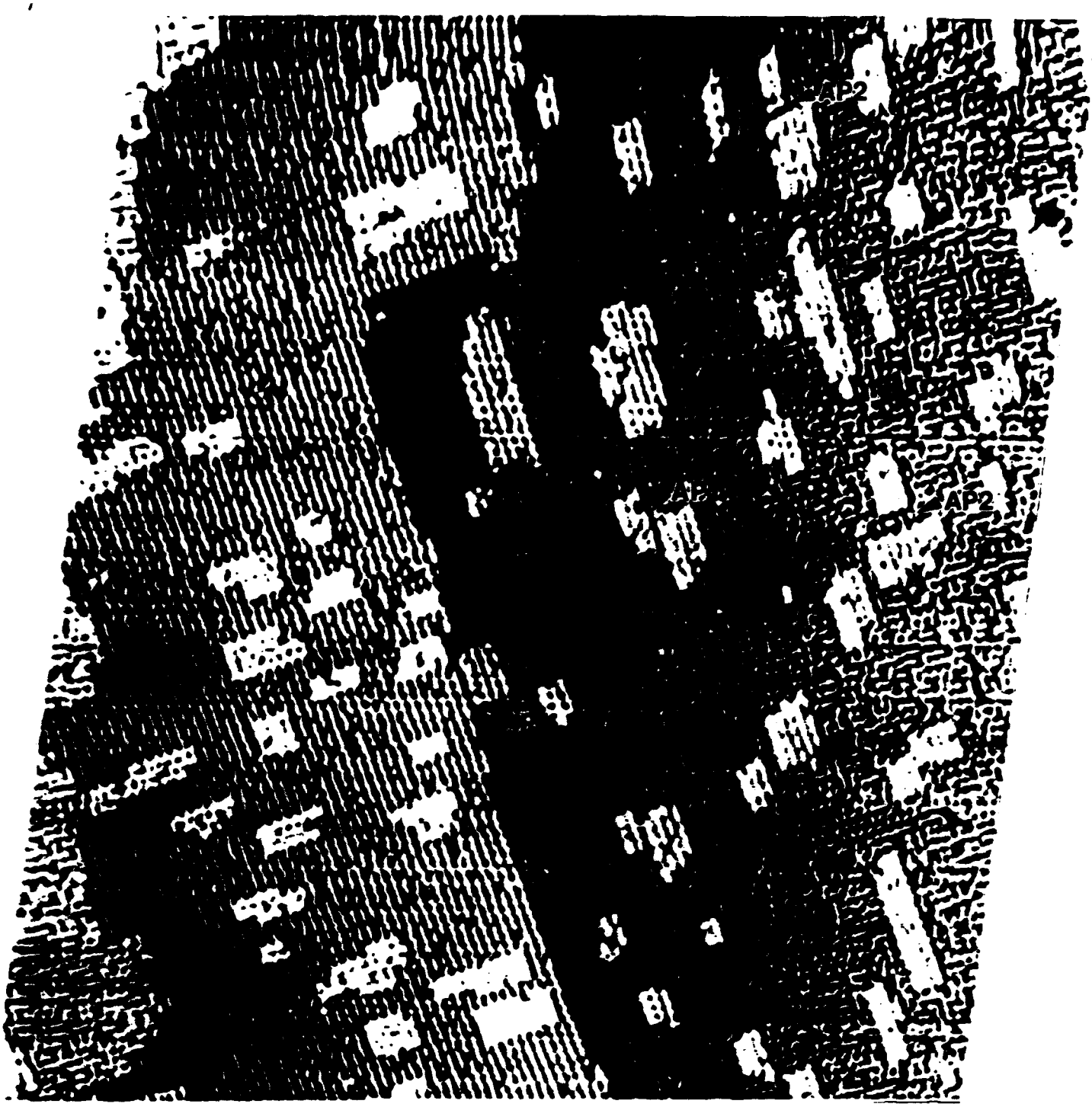

Wang et al

Fig. 23

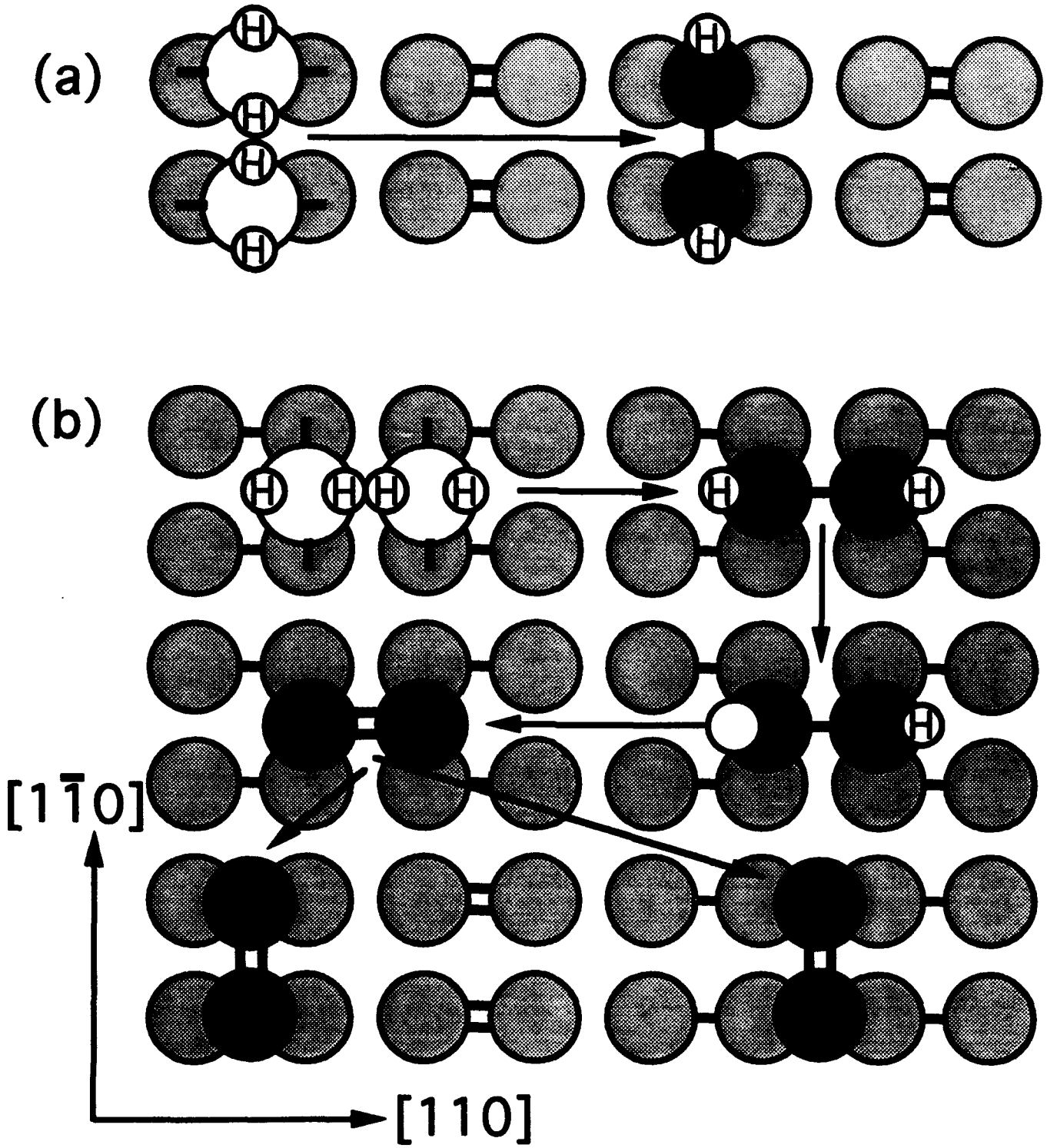

(Wang et a
Fig. 24